Biomaterials Advances 182 (2026) 214698

Contents lists available at ScienceDirect

Biomaterials Advances

journal homepage: www.journals.elsevier.com/materials-science-and-engineering-c

Engineering of green sterilization technology to obtain biocompatible aerogels: Supercritical CO_2 versus ethylene oxide and gamma radiation

María Carracedo-Pérez [a], Antonella Caterina Boccia [b], Inés Ardao [c], Cláudia P. Passos [d], Víctor Santos-Rosales [a], Beatriz Santos [e], Fabio Bernardo [f], María Blanco-Vales [a], Beatriz Magariños [e], Carlos A. García-González [a,*]

[a] AerogelsLab, I+D Farma Group (GI-1645), Department of Pharmacology, Pharmacy and Pharmaceutical Technology, Faculty of Pharmacy, iMATUS and Health Research Institute of Compostela, E-15782, Spain
[b] Institute of Chemical Sciences and Technologies-SCITEC "G. Natta", CNR-National Research Council, Via A. Corti, 12, 20133, Milano, Italy
[c] BioFarma Research Group, Department of Pharmacology, Pharmacy and Pharmaceutical Technology, Innopharma Drug Screening and Pharmacogenomics Platform, Centro Singular de Investigación en Medicina Molecular y Enfermedades Crónicas (CiMUS), Universidade de Santiago de Compostela, Santiago de Compostela E-15782, Spain
[d] LAQV-REQUIMTE, Department of Chemistry, Universidade de Aveiro, 3810-193, Aveiro, Portugal
[e] Department of Microbiology and Parasitology, Aquatic One Health Research Center (iARCUS), Faculty of Biology, CIBUS, Universidade de Santiago de Compostela, Santiago de Compostela, 15782, Spain
[f] CICECO, Department of Chemistry, Universidade de Aveiro, 3810-193, Aveiro, Portugal

ARTICLE INFO

Keywords:
Bioaerogels
Supercritical fluids
Sustainable processing
Sterilization
qNMR spectroscopy

ABSTRACT

The growing relevance of aerogels in biomedicine demands the choice of compatible sterilization techniques with these materials. Conventional methods, such as ethylene oxide (EO) and gamma radiation (γ-rays) sterilization, have significant drawbacks while facing important environmental restrictions. In this study, supercritical CO_2 ($scCO_2$) sterilization is tested for polysaccharide (starch and alginate) aerogels as an eco-friendly alternative to conventional procedures. Three post-processing treatments under different CO_2 exposure regimes (static, dynamic and combined) and in the presence of H_2O_2 as additive were developed and assessed to reach sterility assurance levels (SAL) below 10^{-6}. After sterilization, a vacuum treatment was implemented to ensure a low residual presence of H_2O_2 in the aerogels so that the material biocompatibility was not compromised according to *in vitro* cell tests with fibroblasts. The residual adsorbed H_2O_2 was quantified for the first time in aerogels by nuclear magnetic resonance spectroscopy. The effects of the supercritical sterilization treatments on the textural and chemical properties of the aerogels were evaluated and compared to those treated with EO and γ-rays. Results highlight the unique efficiency of $scCO_2$ sterilization as a post-processing method that preserves the aerogel structure while offering an eco-sustainable potential for producing sterile and biocompatible materials.

1. Introduction

Innovative porous biomaterials are engineered as scaffolds for regenerative medicine to address the clinical challenges of rejections, biomechanical mismatch, and surgical infection risks associated with allografts and synthetic implants [1]. Namely, aerogels stand out as a special category of nanoporous biomaterials characterized by their light weight, high specific surface area and open mesoporosity [2]. Their high porosity provides them bioactive properties, in some cases mimicking the extracellular matrix of biological tissues [3,4] and can also be used as carriers for delivery of various therapeutic agents such as antibiotics [5], antineoplastic [6] and antibacterial [7] agents. They can be produced in a variety of morphologies and from a wide range of sources, being natural polymers (e.g., polysaccharides) of special interest for biomedical purposes due to their biocompatibility and biodegradability.

Healthcare-associated infections (HAIs) are an important challenge in hospitals. It was estimated that *ca.* 17 % of HAIs in the United States were due to surgical site infections, and 55 % could have been prevented [8]. Surgical site infections are also responsible for the rejection of implants which may require subsequent corrective surgery and/or lead to therapeutic failure [8,9]. Consequently, sterility assurance of supplies and aseptic clinical practices are essential within infection prevention

* Corresponding author.
E-mail address: carlos.garcia@usc.es (C.A. García-González).

https://doi.org/10.1016/j.bioadv.2025.214698
Received 19 November 2025; Received in revised form 18 December 2025; Accepted 30 December 2025
Available online 2 January 2026

protocols. The Sterility Assurance Level (SAL) is defined as the probability that a product would remain contaminated after undergoing a sterilization process. Regulatory standards specified for implantable medical devices recommend SAL below 10^{-6} (denoted as SAL-6), i.e., at most, there is a one in a million chance that a viable microorganism survives the said sterilization process [10].

The development of a sterilization technique able to reach SAL-6 and compatible with polymeric materials of intricate geometries, such as aerogels, is urgent [11]. Depending on the properties of the material to be sterilized, the most widely used sterilization techniques in industry include steam sterilization, ethylene oxide (EO) and gamma radiation (γ-rays), but are typically not compatible with aerogels. Steam sterilization is based on microbial inactivation by thermal and moist effects, typically using 121 °C, 1.1 bar and an exposure time of 20 min [12]. Even though this technique is cost-effective, it is not compatible with heat-sensitive materials, such as thermolabile polymers or biopolymer-based materials [11,13,14]. Sterilization with EO may be effective for thermolabile materials, as it operates at moderate temperatures (*ca.* 55–60 °C) [15], but high safety operating procedures are required due to high toxicity and carcinogenicity of this chemical additive [15–17]. Finally, γ-rays can induce modifications in the physicochemical properties of the biomaterials exposed [18], but also the genetic material of the surrounding living beings. Due to the environmental and health concerns about EO and γ-rays, international regulations are being revised to impose stricter limitations to these methods [15,16,19,20].

The United States Food and Drug Administration (FDA) has identified carbon dioxide under supercritical conditions ($scCO_2$) as an innovative alternative for sterilization [11,21–23]. The operational conditions of $scCO_2$ must be set above its critical point (31.1 °C and 73.7 bar), where CO_2 exhibits intermediate properties between liquid and gas, without leaving toxic residues. The inactivation mechanism of this technique lies in the bactericidal nature of CO_2, which is considered as a GRAS (*Generally Recognized as Safe*) substance [11,24]. Moreover, this technique valorizes CO_2, a by-product of several industrial processes, thus promoting the reduction of the carbon footprint.

Several protocols have been developed to inactivate viruses [25], bacterial suspensions [22,24] and bacteria endospores [26,27] based on the efficacy of $scCO_2$. Although this sterilization technique is not yet integrated into the industrial environment, the $scCO_2$ process showed promising results in preserving the physical integrity of aerogels [27]. Obtaining sterile aerogels is possible directly from the wet gel by integrating the sterilization process within the drying process [27]. This method contributed to shorter process durations and minimized handling steps. However, sterilizing already manufactured aerogels remains challenging, since their porous architecture and chemical composition are highly sensitive. This situation becomes critical when aerogels have to be incorporated into formulations together with non-sterile components (i.e. drugs, other excipients, fabrics), where the whole final product must be sterile.

Given its proven effectiveness in microbial inactivation and its mild operating conditions, $scCO_2$ is emerging as a promising sterilization method for highly sensitive materials such as polysaccharide aerogels. To the best of our knowledge, the feasibility of $scCO_2$ as a post-manufacturing sterilization strategy while preserving the physicochemical and biocompatible properties of starch aerogel cylinders and alginate aerogel beads was herein assessed for the first time. The $scCO_2$ sterilization treatment was developed and optimized in terms of exposure time (from 2 to 5 h), hydrogen peroxide (H_2O_2) additive concentration (0, 670 and 1330 ppm or mg/L), processing regime (static, dynamic and combined) and aeration treatment (vacuum and exposure to CO_2 atmosphere). Alternatively, the same untreated aerogels were sterilized by EO and γ-rays treatments following standardized protocols for the sake of comparison. Textural properties of the sterilized aerogels were compared in terms of porosity, specific surface area, main pore diameter and specific pore volumes with those of the untreated samples. The porous structure was also assessed by scanning electron microscopy (SEM). The chemical nature of both polysaccharide aerogels was evaluated by Fourier-Transform Infrared (FTIR) analysis, and the amylose-to-amylopectin ratio of starch aerogels was also enzymatically quantified. For the first time, quantitative proton nuclear magnetic resonance spectroscopy (^{1}H qNMR) was also employed to simultaneously analyze possible changes in the chemical structure of the aerogels and quantify H_2O_2 content present in aerogels sterilized by the $scCO_2$ treatment. Moreover, starch and alginate chemical properties were assessed by gel permeation chromatography (GPC). For potential biomedical use purposes, the sterile aerogels were assessed with cytotoxicity tests using NIH-3T3 cell line at two different timepoints (24 and 48 h).

2. Materials and methods

2.1. Materials

Native maize starch (SP, Amylo N-460, 52.6 % amylose content, 12.9 % loss on drying, conform to USP and EP, <1 wt% protein, according to the supplier) was provided by Roquette Frères S.A. (Lestrem, France). Alginic acid sodium salt from brown algae (guluronic/mannuronic acid ratio of 70/30, Mw = 403 kDa) was supplied by Sigma Life Science (Irvine, UK) and calcium chloride anhydrous ($CaCl_2$, >99 % purity) provided by Scharlab (Barcelona, Spain) was used as Ca^{2+} crosslinker source. Absolute ethanol (EtOH, >99.9 % purity) and CO_2 (99.8 % purity) were supplied by VWR (Radnor, PA, USA) and Nippon Gases (Madrid, Spain), respectively. Hydrogen peroxide (H_2O_2) 30 % (w/w) was supplied by Sigma-Aldrich (Madrid, Spain). Water was purified using reverse osmosis (resistivity >18 MΩ·cm, Milli-Q, Millipore®, Madrid, Spain).

Sterility biological indicator was *Bacillus pumilus* (ATCC 27142) spore strips (10^6 spores/strip) purchased from Sigma-Aldrich (Madrid, Spain). Trypticase soy agar (TSA) and broth (TSB) media were purchased from BIOKAR Diagnosis (Pantin, France). Ultrapure nitrogen (N_2 > 99 % purity) supplied by Nippon Gases (Madrid, Spain) was used for the adsorption-desorption textural analysis. The amylose-to-amylopectin ratio was determined by using an enzymatic test kit 138 (K-AMYL) purchased from Megazyme (Wicklow, Ireland). Prior to the GPC tests, alginate samples were pretreated with dimethyl sulfoxide (DMSO, 99.978 % purity) provided by Fisher Scientific (Loughborough, UK). For the ^{1}H qNMR analyses, deuterated water (D_2O) or deuterated dimethylsulfoxide (*d*-DMSO) provided from CortecNet (Les Ulis, France), and H_2O_2 35 % w/w from Merck (Milano, Italy) were used.

2.2. Aerogels production by $scCO_2$ technology

Starch cylindrical and alginate beads hydrogels were prepared following a reported methodology [27]. Briefly, cylindrical starch hydrogels were prepared from aqueous 8 % (w/w) starch dispersions. The solutions were dosed in cylindrical syringes (50 mm in height and 10 mm in diameter). After being stored at 4 °C for 48 h for retrogradation, the starch hydrogels were immersed in EtOH to obtain alcogels and 24 h later the alcogels were cut into cylinders of 3.5 mm length. Alginate hydrogel beads were prepared using the dripping method by ionic gelation of a 2.0 % (w/w) solution dropped through a syringe (2 mm nozzle diameter) on an aqueous 150 mM $CaCl_2$ solution bath. After 2 h of aging in the $CaCl_2$ solution under constant stirring, the hydrogel particles were directly submerged in absolute EtOH for solvent exchange to obtain alcogel beads. Both polysaccharide alcogels were subjected to two additional solvent exchange steps at 24 and 48 h to completely replace the water with EtOH in the gel structure (Fig. 1).

The resulting starch and alginate alcogels were enclosed in filter paper pouches and subjected to a supercritical drying treatment. The supercritical drying was performed in a manual equipment (HPE-350 lab, Eurotechnica GmbH, Bargteheide, Germany) provided with an extractor of 400 mL of operative volume. The samples were placed inside the high-pressure vessel and soaked with 80 mL of EtOH. The

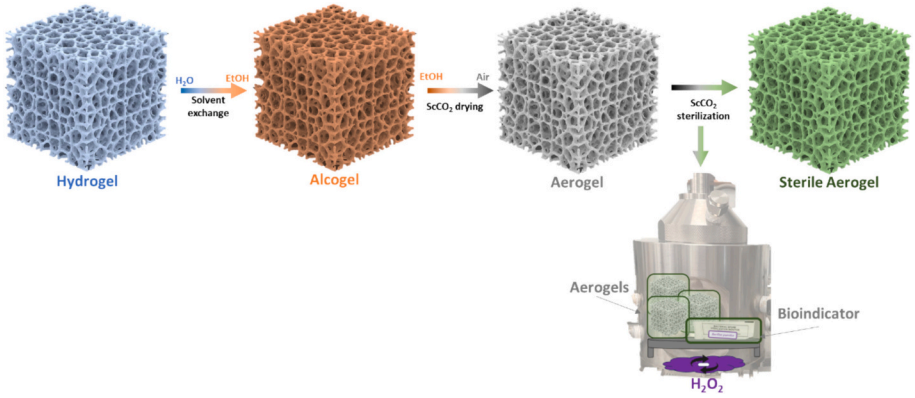

Fig. 1. Schematic representation of the process used to obtain $scCO_2$-sterilized aerogels. The fabricated hydrogels were directly immersed in absolute ethanol to obtain alcogels, which were subsequently converted into aerogels by $scCO_2$ drying. The aerogels were then placed in a high-pressure vessel with H_2O_2 loaded at the bottom of the autoclave, and alongside *B. pumilus* bioindicator spore strips, to achieve $scCO_2$-sterilized aerogels.

process was carried out at 39 °C under three consecutive steps at different operating conditions: (1) a constant flow rate of 15 g/min of CO_2 at 120 bar during 2 h; (2) a step at 135 bar without flow for 1 h; and (3) a flow rate of 7 g/min of CO_2 at 120 bar for 1.5 h. Finally, the autoclave was manually depressurized at a rate of 1.5 bar/min.

The prepared starch (samples named as *STA*) and alginate (samples named as *ALG*) aerogels were packaged in thermosealed sterilization pouches (Soplaril Hispania, Barcelona, Spain) to avoid contamination after being subjected to the different sterilization protocols.

2.3. Development and optimization of the $scCO_2$ sterilization protocol for polysaccharide aerogels

The sterilization treatment consisted of evaluating the survival resistance of *B. pumilus* dry spore strips to a $scCO_2$ environment at 140 bar and 39 °C, under constant stirring (700 rpm) and establishing a depressurization rate of 3 bar/min. Each sterilization treatment was performed in triplicate. The dried spore strips were packaged in thermosealed sterilization pouches, placed in a 100 mL high-pressure vessel (TharSFC, Pittsburg, PA, USA) and subjected to sterilization conditions. After sterilization, the spore strips were collected and seeded in TSB medium and incubated for 7 days at 37 °C. The test of absence of bacterial growth was carried out by naked-eye evaluation of the turbidity in the tubes and confirmed by seeding on TSA plates each day for 7 days. The processing conditions were considered sterilizing at SAL-6 sterilization levels when there was absence of bacterial growth for these strains after 7 days of culture.

The effects of exposure times (2–5 h), H_2O_2 concentrations (0–1330 ppm or mg/L) and the operating regime for the renewal of the $scCO_2$ environment inside the autoclave during sterilization (*static, dynamic* and *combined*) on sterilization efficacy were tested to identify the optimal conditions. In the *static regime,* $scCO_2$ was maintained inside the autoclave without any fresh CO_2 flow. In the *dynamic regime*, a continuous flow of fresh CO_2 at 5 g/min was used to renew the autoclave environment. Finally, a *combined regime* was tested, integrating both static and dynamic conditions, with durations ranging from 1 to 2.5 h, for the static, and 1.5–2.5 h for the dynamic, respectively. Accordingly, the batch trial conditions were denoted as ***$ScCO_2$Regime_Time_Concentration:*** where *Regime* corresponds to static (*St)*, dynamic (*Dy)*, or combined (*Co)* regimes; *Time* is the exposure time (1, 2, 2.5, or 5 h). In the case of the samples obtained by the combined regime, the *Time* is expressed as *static duration + dynamic duration*. Finally, *Concentration* is the H_2O_2 concentration used (0, 670, or 1330 ppm).

The most effective sterilization conditions for each regime (i.e. the lowest processing time and additive concentration combination) were applied to starch and alginate aerogels, yielding the following designations: *STA_scCO₂St* and *ALG_scCO₂St* (static), *STA_scCO₂Dy* and *ALG_scCO₂Dy* (dynamic), and *STA_scCO₂Co* and *ALG_scCO₂Co* (combined).

Selected $scCO_2$ sterilized samples (*STA_scCO₂Co* and *ALG_scCO₂Co*) were subsequently subjected to different aeration treatments (vacuum or exposure to CO_2 atmosphere): 1) Vacuum (−0.8 mbar) treatment during different times (2–24 h) at room temperature; samples denoted as *STA_scCO₂Co_Vt* and *ALG_scCO₂Co_Vt,* where *t* is the vacuum duration. 2) Exposure to fresh CO_2 atmosphere at different pressures (2.5 or 50 bar) for 3 h; samples denoted as *STA_scCO₂Co_ xbar* and *ALG_scCO₂Co_xbar,* where *x* can be *2.5* or *50* depending on the pressure (in bar) used. The aerogel samples were subjected to aeration enclosed in the same thermosealed sterilization pouches previously used during the sterilization procedure and without any manipulation.

2.4. Conventional sterilization procedures tested on polysaccharide aerogels

2.4.1. Ethylene oxide: chemical sterilization treatment

EO sterilization process was carried out in a SUOD142483 sterilizer (Suphatec S.L., Bigues i Riells, Spain) by Esterilización S.L. (Barcelona, Spain) following the ISO 11135:2014 [28]. The aerogel samples in thermosealed pouches were treated under 55 °C and a minimum relative humidity of 40 % for 4 h. Then, sequential ventilation steps were performed as follows for cleaning possible toxic EO residues in the samples. Firstly, the samples were subjected to a vacuum process for 21 min, followed by a fresh N_2 flow for 8 min at 600 mbar. Then, a second vacuum period of 12 min was carried out, followed by an 8-min air venting step at 600 mbar. The samples were ventilated with fresh air at 500 mbar for 34 min and could be collected 48 h after. The obtained samples were denoted as *ALG_EO* and *STA_EO*.

2.4.2. γ-Rays: physical sterilization treatment

Polysaccharide aerogel samples in thermosealed pouches were delivered to a first-category radioactive institution IR/B-02/69 (Aragogamma S.L., Les Franqueses del Vallès, Spain) to be subjected to γ-ray irradiation. The treatment was performed with a ^{60}Co source reaching a dose of 30.6 kGy and exposing the material for 7.53 h, following the ISO 11137-A2:2020 [29]. The obtained samples were denoted as *ALG_γ-rays* and *STA_γ-rays*.

2.5. Textural characterization of aerogels

The bulk density of starch aerogel cylinders (ρ_{Bulk}) and the envelope density of the alginate aerogel beads (ρ_{Env}) were determined from the density equation. The volume of the starch aerogels was calculated by measuring the diameter and the height of the cylinders. The particle

diameter of alginated aerogel beads was measured by a dynamic image analysis using a CamSizer X2 (Microtrac Retsch GmbH, Haan, Germany). This equipment equipped with an X-Fall module allowed a controlled amount of sample to be introduced into the feeding system to ensure a continuous and uniform flow through the detection zone which employs a dynamic image acquisition using high-speed cameras to detect particles in the diameter size range of 0.8 μm to 8 mm. For each sample, at least 100 particles were measured. The analysis was conducted using the MICROTRAC software (Microtrac Retsch GmbH, Haan, Germany) measuring particles with sphericities higher than 0.7.

The skeletal density of the aerogels (ρ_{Skel}) was determined using a helium pycnometer (Quantachrome, Boynton Beach, FL, USA) at room temperature (25 °C) and 1.01 bar. Values were obtained from five replicates (standard deviation <5 %). The resulting overall porosity (ε) was calculated according to Eq. (1), where ρ_i corresponds to either bulk or envelope density.

$$\varepsilon(\%) = \left(1 - \frac{\rho_i}{\rho_{Skel}}\right) x\,100 \quad (1)$$

The shrinkage (S_V) of the treated materials was calculated in terms of volume following Eq. (2) by comparing the volume of the untreated aerogel (V_{Blank}) and the aerogel after being subjected to different sterilization treatments ($V_{Treated}$).

$$S_V(\%) = \frac{V_{Blank} - V_{Treated}}{V_{Blank}} \quad (2)$$

The textural properties of the untreated and sterilized aerogels were determined by N_2 adsorption-desorption analysis (ASAP 2000 Micromeritics Inc., Norcross, GA, USA). Firstly, the samples were degassed under vacuum (<1 mPa) for 24 h with a degassing temperature of 40 °C and 60 °C for alginate and starch aerogels, respectively. The specific surface area (A_{BET}) of the aerogels was determined by the Brunauer-Emmett-Teller (BET) method, whereas the Barrett-Joyner-Halenda (BJH) method was used to calculate the specific pore volume (V_P), the percentages of the specific mesopore volume (V_{meso}) and specific macropore volume (V_{macro}), and mean pore diameter (D_P) from the data of the desorption branch of the N_2 adsorption-desorption isotherm.

Moreover, the samples were sputter-coated with a 10 nm layer of iridium (Q150 T S/E/ES equipment, Quorum Technologies, Lewes, UK) and studied by scanning electron microscopy (SEM) using a FESEM UltraPlus microscope (Zeiss, Jena, Germany).

2.6. Chemical characterization of aerogels

The chemical properties of starch and alginate raw materials (*Raw powder*), the untreated (*Blank*) and the sterile aerogel samples were characterized to identify any changes arising from the different sterilization processes. FTIR measurements were carried out on a Bruker Tensor 27 (Bruker Optics, Inc., Billerica, MA, USA) spectrometer, on KBr disc, by mixing 1 mg of dried sample with an appropriate amount of KBr, until free of granularity. The spectra were recorded within the 4000–400 cm^{-1} wavenumber range.

Monodimensional NMR experiments were recorded on a Bruker AVANCE NEO 600 spectrometer (Bruker Biospin, GmbH Rheinstetten, Karlsruhe, Germany, with Bruker Bio-spin software TOPSPIN v.4.1.4), operating at 14.07 T, equipped with a 5 mm reverse Z gradient cryoprobe Prodigy, and thermostated autosampler at 320 K. The preparation of samples for the NMR analysis, and the acquisition and processing parameters are described in Supplementary Information (section *SI 1.1*).

The chemical structure of the starch aerogels was also evaluated by determining the amylose-to-amylopectin ratio using the enzymatic test kit K-AMYL. The untreated and sterilized samples were weighed (*ca.* 17.5 mg) and ground with a mortar to obtain a powder. To avoid the interference of lipid contents, the samples were pre-treated by dispersing in 1 mL DMSO using a vortex mixer, heated in boiling water for 15 min, and cooled at room temperature for 5 min. Subsequently, 2 mL of EtOH 95 % (V/V) were added under continuous stirring to precipitate the defatted starch. A pellet was obtained after centrifuging at 2,000 rpm (Compact Tabletop Centrifuge 2010, Kubota, Tokyo, Japan) for 5 min and dispersed in 2 mL DMSO using a vortex mixer and heated in water for 15 min. A 4 mL solution of concavalin A (Con A) which forms complexes with amylopectin solution, was added and vigorously mixed, transferred to 25 mL volumetric flask and diluted with the previous Con A solution. The following steps, according to the kit procedure, include the determination of total starch, precipitation of amylopectin (after denaturation of Con A), and determination of amylose remaining content. The amylose content is then calculated according to Eq. (3), where 6.15 and 9.2 are the dilution factors for the Con A and Total Starch extracts, respectively. Each sample was measured with two or three (if the average deviation was >5 %) replicates.

$$Amylose\ (\%w/w) = \frac{6.15 \cdot Abs_{Con\ A\ supernatant}}{9.2 \cdot Abs_{Total\ Starch}} \cdot 100 \quad (3)$$

The number-average (Mn), weight-average (Mw) molecular weights of both polysaccharide aerogels, along with the polydispersity index (Đ = Mw/Mn), as well as the degree of polymerization (DP) were determined using an absolute multi-angle laser light scattering (MALS) detector connected to a size-exclusion chromatographic system. The analysis of the alginate aerogels was performed using a Malvern Panalytical system (Malvern, UK) equipped with two PL aquagel-OH MIXED 8 μm (300 × 7.5 mm) columns, preceded by a PL aquagel-OH Guard 8 μm (50 × 7.5 mm) pre-column. Data acquisition and processing were carried out using OMNISEC v11.41 software (Malvern, UK). The refractive index detector and the columns were maintained at 40 °C, while the autosampler was held at 35 °C. The eluent (0.1 M $NaNO_3$ in water) was delivered at a flow rate of 0.9 mL/min. Calibration was performed using pullulan standards (Polymer Laboratories, Shropshire, UK) in the 5.8–380 kDa molecular weight range. Samples were prepared by dissolving the polymer in 0.1 M $NaNO_3$ aqueous solution at 25 °C for 60 min to a final concentration of 2–4 mg/mL, followed by filtration through a 0.22 μm PTFE membrane filter.

2.6.1. H_2O_2 quantification on $scCO_2$ sterilized aerogels

The quantification of H_2O_2 was done acquiring ^1H qNMR spectra and the concentration of H_2O_2 was calculated from Eq. (4), where $[mM]_{HD}$ and $[mM]_S$ are the concentrations of H_2O_2 (in mM) and the standard solution, respectively; I_{HD} and I_{st} are the integrals values and H_{HD} and H_S the number of protons estimated from the signal of H_2O_2 and the standard solution, respectively [30,31].

$$[mM]_{HD} = \frac{I_{HD}}{H_{HD} \cdot [mM]_S} \cdot \frac{H_S}{I_S} \quad (4)$$

Eq. (4) is based on the assumption that the peak areas are directly proportional to the number of nuclei responsible for the corresponding signals, in the active volume. Data was acquired on two slots of samples and in triplicate to validate the reproducibility of both experimental synthesis and NMR data. The solvent peak (d-DMSO) was normalized in all spectra, and the reference standard with the closest matching H_2O_2 signal to the sample was selected. The area of the H_2O_2 signal was quantified using an external standard solution of H_2O_2 in d-DMSO, selected within a series of known H_2O_2 concentrations solutions (Table S1 in Supplementary Information).

To validate this ^1H qNMR method, H_2O_2 quantification was also assessed with an internal standard solution. Toluene was chosen as the internal standard because it is chemically inert with the functional groups of both polysaccharides, and its ^1H NMR resonances do not overlap with those of starch and alginate. Furthermore, toluene is available in high purity and is soluble in DMSO. The H_2O_2 content was determined comparing the integral of H_2O_2 with those of the aromatic resonances of toluene (7.25–7.15 ppm), in Eq. (4), and considering a 6.27 mM concentration for the internal standard.

2.7. Cell viability studies

The cytocompatibility of the sterilized aerogels was tested with the NIH-3 T3 cell line (ATCC: CRL-1658) [5]. The cells were seeded in 24-well plates containing 500 μL DMEM supplemented with 10 % bovine serum and 1 % penicillin-streptomycin (12000 cell per cm^2 for 24 h and 8000 cell per cm^2 for 48 h) and incubated at 37 °C in a humidified atmosphere supplemented with 5 % CO_2. After 24 h, the materials were placed in 24-well culture inserts (PET track-etched membrane with 0.4 μm pore size) in triplicate, 100 μL of medium was added on top and they were introduced in the well plate. To ensure that potential H_2O_2 residues will be dissolved in the medium, the viability was also measured in triplicate after 48 h. Negative controls consisting of cells without material were also incubated under the same conditions and in triplicate for 24 and 48 h. The untreated aerogels (*Blank*) were firstly sterilized by UV for 30 min and then placed in the wells with cells using culture inserts.

Cell viability was assessed using the resazurin assay that measures the mitochondrial function of metabolic active cells. The material was removed from the cells after 24 and 48 h of incubation; the culture medium was aspirated and 300 μL of 44 μM resazurin were added in each well. After 3 h of incubation under identical conditions, fluorescence was measured at an excitation wavelength of 544 nm and an emission wavelength of 590 nm in a microplate reader (Infinite® M200, Tecan Group Ltd., Männedorf, Switzerland).

2.8. Statistics analysis

Results were expressed as mean ± standard deviation. Statistical analyses of textural properties, amylose-to-amylopectin ratio results and cell viability were obtained using 2-way ANOVA test ($p < 0.05$) followed by the post-hoc Tukey HDS multiple comparison test using GraphPad Prism v.8.0.2 (GraphPad Software, Boston, MA, USA).

3. Results and discussion

3.1. Development of $scCO_2$ sterilization treatments under different exposure regimes

Microbial inactivation using $scCO_2$ technology positions itself as a sustainable alternative to the environmental and operational hazards encountered with EO and γ-rays [15,16,18,19]. The $scCO_2$ sterilization method also allows the valorization of the abundant CO_2 generated as a by-product in various industrial processes. Following the standardized sterilization models used for EO and γ-irradiation, a biological indicator was employed to verify the efficacy of the process [28,29]. For supercritical sterilization, the most resistant type of microorganism (bacterial endospores) was selected. Extensive studies demonstrated that *B. pumilus* is the most resistant bioindicator [26,27,32,33]. Accordingly, a complete inactivation of the biological indicator with a probability of one surviving organism in one million (SAL-6) ensures that weaker vegetative bacteria, both Gram-positive and Gram-negative, and fungi can be considered fully inactivated [26]. Aiming the standardization of this sterilization technology, dry endospores of *B. pumilus* were demonstrated as the most resistant microorganism and thus established as biological indicator (BI) for this technique [27,32,33]. Microbiological inactivation using $scCO_2$ without additives has been demonstrated in numerous studies, but always without reaching SAL-6 against *B. pumilus* dry bacterial endospores [24,34,35]. The effectiveness of water as an additive of $scCO_2$ has been reported for enhancing the inactivation of *B. pumilus* in a liquid suspension, which is a weaker form than dry spores, and under working conditions (200 bar, 55 °C for 1 h) not compatible for the treatment of aerogels and thermosensitive materials [36,37]. This BI was only reliably sterilized in $scCO_2$ environments by adding oxidants such as H_2O_2 or peracetic acid (PAA) [26,27,32,34,38–40]. This type of additives acts by generating hydroxyl radicals that disrupt key cellular components, including DNA and membrane lipids [41,42]. Compared to PAA, H_2O_2 offers important advantages such as being odorless, less corrosive, and decomposing into harmless water and oxygen, thereby reducing toxic residues and improving material compatibility [43]. Nevertheless, residual H_2O_2 must be carefully controlled in the sterilized material due to its cytotoxicity and negative effects on tissue compatibility above threshold levels [44,45].

The process parameters involved in the $scCO_2$ sterilization treatment are numerous and a multivariable study involving a significant experimental effort is required to define the optimum conditions. To reach the mildest sterilant conditions, the working pressure, temperature, stirring and depressurization rates were set at 140 bar, 39 °C, 700 rpm, and 3 bar/min, respectively, based on previous results in literature [26]. The new protocols of $scCO_2$ sterilization herein presented are based on three different exposure regimes: *static*, *dynamic* and *combined*. In the *combined* regime, tests were designed with a first *static* regime step, followed by a *dynamic* regime step. The combined regime encompasses the advantages of working on batch [34] that ensures a contact of the material with a known additive content for a certain time, and of working in continuous that favors the removal of the additive entrained with a fresh CO_2 flow and the extraction of cell membrane components by extraction, thus enabling enough time for sterilization to be completed while removing the additive within the process [27]. The two other processing parameters were exposure duration and H_2O_2 concentration. The optimization of the protocol in terms of process duration will reduce economic costs, whereas the reduction of the H_2O_2 presence during the procedure will favor the biocompatibility of the material.

All conducted sterilization tests are presented in Table 1. Sterilization efficacy was evaluated using commercial dry-spore strips containing 10^6 spores. After incubation in TSB and TSA media for 7 days, the absence of microbial growth corresponds to a log-6 reduction, confirming sterility. A 5-h treatment applied under static, dynamic, or combined (2.5 + 2.5 h) regimes, enabled the complete spore inactivation even at H_2O_2 concentrations of 670 ppm. In contrast, shorter treatments (2 h) failed to achieve sterility. Also, 670 ppm of H_2O_2 was insufficient within 2.5 h of exposure. In all cases, since the H_2O_2 solution consists of a H_2O_2:H_2O mixture of 30:70 (w/w), the addition of 1330 ppm of H_2O_2 inherently includes a proportional amount of H_2O (3110

Table 1
Sterilization experimental trials under $scCO_2$ against *B. pumilus* dry bacterial endospores. Conditions in bold text correspond to the selected optimized conditions.

Trial	Regime	Duration (h)	H_2O_2 (ppm)	*B. pumilus* sterility
$scCO_2$St_5_1330	Static	5	1330	YES
$scCO_2$Dy_5_1330	Dynamic	5	1330	YES
$scCO_2$Co_2.5+2.5_1330	Combined (Static+Dynamic)	2.5 + 2.5	1330	YES
$scCO_2$St_5_670	Static	5	670	YES
$scCO_2$Dy_5_670	Dynamic	5	670	YES
$scCO_2$Co_2.5+2.5_670	Combined (Static+Dynamic)	2.5 + 2.5	670	YES
$scCO_2$St_2.5_1330	**Static**	**2.5**	**1330**	**YES**
$scCO_2$Dy_2.5_1330	**Dynamic**	**2.5**	**1330**	**YES**
$scCO_2$Co_1+1.5_1330	**Combined(Static + Dynamic)**	**1 + 1.5**	**1330**	**YES**
$scCO_2$St_2.5_670	Static	2.5	670	NO
$scCO_2$Dy_2.5_670	Dynamic	2.5	670	NO
$scCO_2$Co_1+1.5_670	Combined (Static+Dynamic)	1 + 1.5	670	NO
$scCO_2$Co_1+1.5_0	Combined (Static+Dynamic)	1 + 1.5	670	NO
$scCO_2$St_2_1330	Static	2	1330	NO
$scCO_2$Dy_2_1330	Dynamic	2	1330	NO
$scCO_2$Co_1+1_1330	Combined (Static+Dynamic)	1 + 1	1330	NO

ppm). An experimental trial was conducted at 0 ppm of H_2O_2 and in the presence of 3110 ppm of pure water (*$scCO_2$Co_1+1.5_0*). This test confirmed that the presence of a strong oxidant additive during the process was necessary, since sterility was not achieved after 2.5 h in the presence of pure H_2O. Overall, the exposure regime itself did not significantly influence the sterilization efficacy, as all three approaches exhibited comparable performances when conducted under similar H_2O_2 contents and duration conditions. The most consistent inactivation result was 2.5 h of treatment with 1330 ppm H_2O_2, regardless of the exposure regime, identifying these conditions as optimal to achieve a complete sterilization of *B. pumilus*.

3.2. Textural characterization of sterilized aerogels

Two polysaccharide (starch and alginate) aerogels were chosen to evaluate the different supercritical sterilization procedures. These materials allow the assessment of the sterility in combination with the material performance, which is crucial for the safe and effective use of polysaccharide-based products in medicine. Starch was selected as a reference material due to their high sensitivity to supercritical conditions [27,46], whereas alginate was chosen for its broad use in regenerative medicine [5,7,24]. In addition, the highly porous and interconnected architecture of aerogels make them interesting model systems for evaluating the textural alterations induced by sterilization. These materials were obtained through $scCO_2$ drying, which is able to

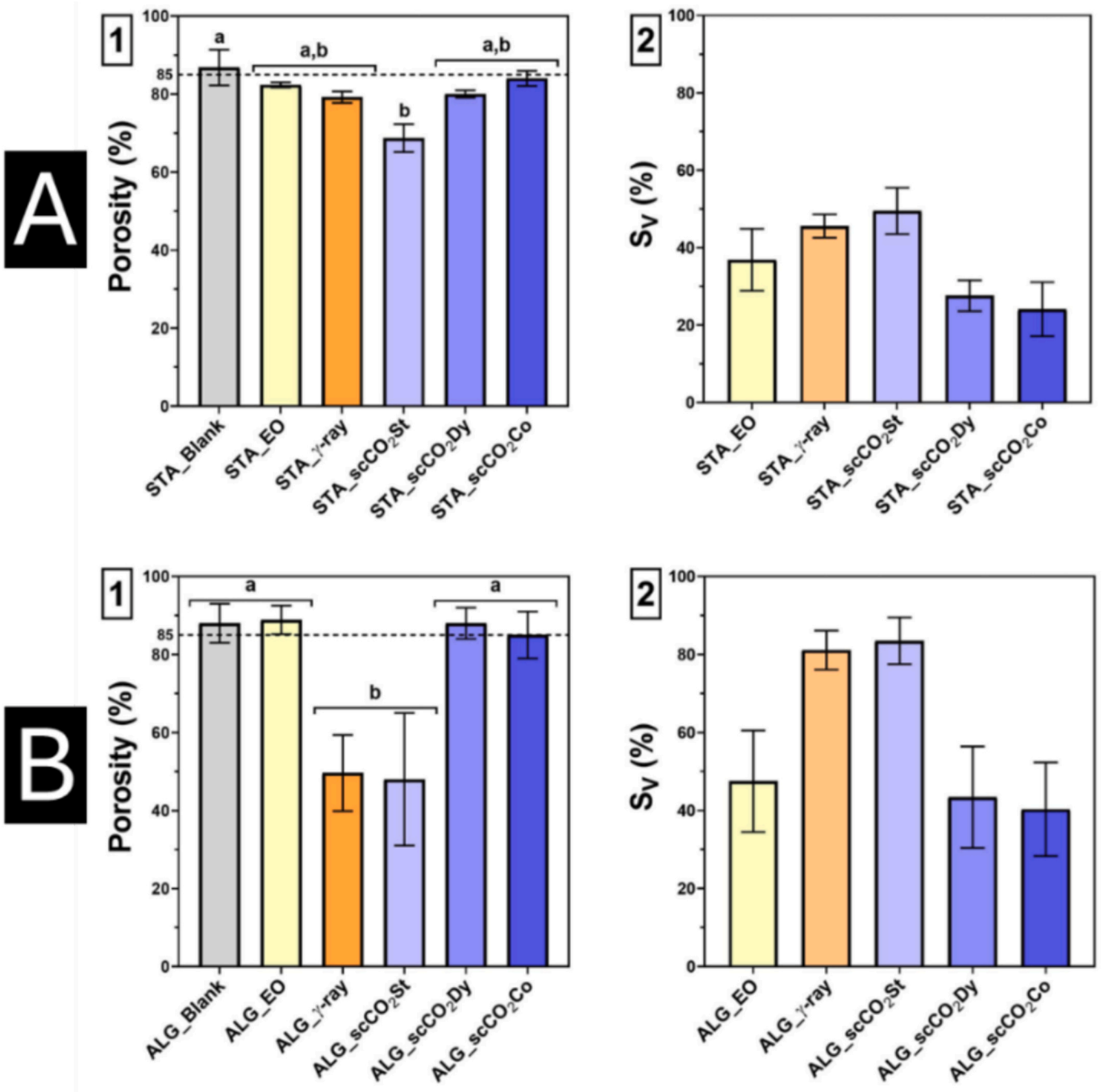

Fig. 2. Textural results of blank and sterilized (A) starch and (B) alginate aerogels: (1) porosity and (2) volume shrinkage (S_V). The dashed line represents the minimum porosity value accepted for aerogels [2,47]. Same letters denoted the same statistic groups.

maintain the 3D porous network of the wet gel intact in the final aerogel regardless of the morphology, a crucial characteristic for the cell adhesion and activity in tissue engineering [2,47,48].

The textural changes induced after the different supercritical sterilization treatments were evaluated by comparing the untreated and the sterile aerogels in terms of porosity and S_V (Fig. 2) as well as A_{BET}, D_P and the distribution of V_P (Fig. 3). Results were also compared to those obtained by EO and gamma sterilization techniques.

After $scCO_2$ drying, blank starch and alginate aerogels (*STA_Blank* and *ALG_Blank*) were characterized, and both presented porosity results (Fig. 2A.1 and B.1) in the range widely accepted for polysaccharide aerogels (≥ 85 %) [2,47]. Sterilized starch aerogels under the *static* $scCO_2$ treatment (*STA_scCO$_2$St*) exhibited significant differences on porosity as well as a 50 % of S_V compared to the untreated sample (*STA_Blank*). The effect of *dynamic* $scCO_2$ treatment (*STA_scCO$_2$Dy*) resulted in porosity values under the accepted range and S_V values of *ca.* 30 %. In contrast, sterilized starch aerogels under the *combined* $scCO_2$ treatment (*STA_scCO$_2$Co*) exhibited a porosity value of *ca.* 85 % and the lowest S_V values. Starch aerogels subjected to conventional sterilization treatments (*STA_EO* and *STA_γ rays*) were below the threshold values of porosity, although there were no statistical differences with respect to the untreated counterpart. Moreover, these aerogels (*STA_EO* and *STA_γ rays*) presented important S_V values, of *ca.* 37 % and 46 %, respectively.

Sterilized alginate aerogels showed relevant differences among the sterilization treatments with respect to the blank for porosity (Fig. 2B.1) and S_V (Fig. 2B.2) values. $ScCO_2$ sterilization had different results depending on the exposure regime used. *ALG_scCO$_2$St* aerogels presented significant textural changes, whereas the use of a flow of fresh CO_2 during sterilization, both in the *dynamic* (*ALG_scCO$_2$Dy*) and *combined* (*ALG_scCO$_2$Co*) regimes, resulted in a non-significant change in porosity of the aerogel. Additionally, the S_V observed in the latter aerogel samples (43.4 % and 40.3 %) were much lower than in *ALG_scCO$_2$St* aerogels. After the EO treatment, no significant changes were observed in the porosity values compared to the *Blank*, and the S_V was also below 50 %. After the γ-rays treatment, the *ALG_ γ-rays* aerogels had a significant decrease in porosity and in S_V (81.1 %).

The results of the N_2 adsorption/desorption analysis (Fig. 3) show that both untreated blank aerogels exhibited A_{BET} values typical for aerogels (≥ 125 m^2/g) [1]. Additionally, the main D_P values confirmed the presence of a mesopore structure, i.e. between 2 and 50 nm, although the predominant pores were in the macropore range [1,2].

The results of the sterilized starch aerogels are shown in Fig. 3A. *STA_scCO$_2$St* aerogels exhibited A_{BET} values under the accepted ones for polysaccharides aerogels, although the D_P and the percentage of V_{meso} were higher than those obtained for the blank sample. This last effect was also observed in starch aerogels sterilized with $scCO_2$ technology in a *static* regime at 245 bar, 40 °C during 6 h in presence of 360 ppm of H_2O_2 [46]. The *static* regime could promote two effects, the collapse of the smaller pores and the solubilization of the water from the additive into the CO_2 environment, thus interacting with the hydrophilic polymeric chains, damaging the aerogel structure [27,49]. On the other hand, the starch aerogel samples treated under a fresh flow of CO_2

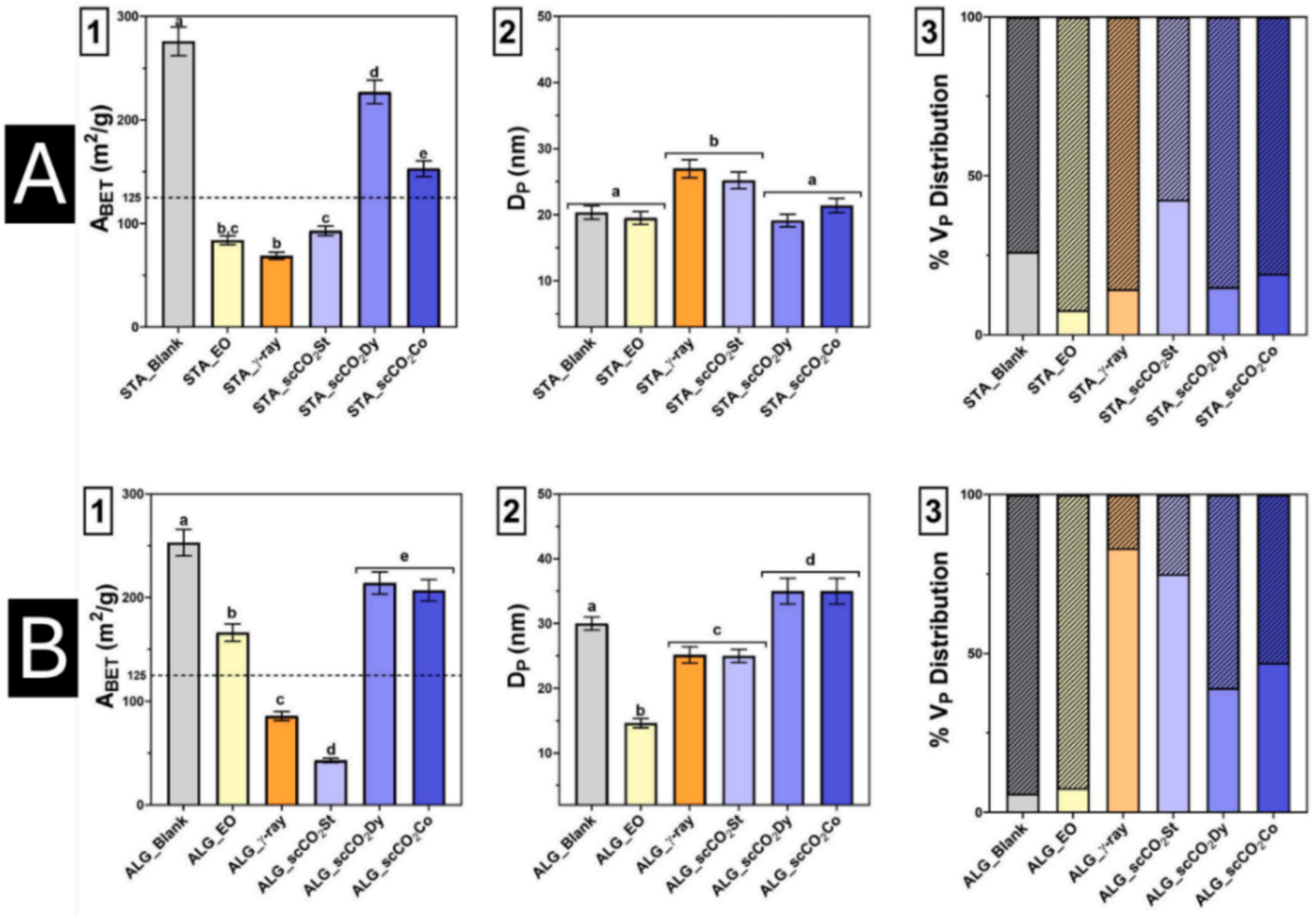

Fig. 3. N_2 adsorption-desorption analysis of (A) cylinders of starch aerogels and (B) beads of alginate aerogels: (1) Specific surface area (A_{BET}); (2) mean pore diameter (D_P) in the range of mesopore (2–50 nm) and (3) pore volume distribution in mesopores (solid bars) and macropores (stripped bars). The dashed line represents the minimum value of A_{BET} widely accepted for aerogels [1]. Same letters denoted same statistic groups.

(*STA_scCO₂Dy* and *STA_scCO₂Co*) exhibited acceptable values on the A_{BET} and D_P, although with a slight increase in the percentage V_{macro} compared to the untreated samples. The samples sterilized with EO (*STA_EO*) did not achieve A_{BET} values within the accepted range for aerogels (Fig. 3A.1). *STA_EO* aerogel exhibited a D_P value within the mesopore range, but the treatment caused a decrease in the percentage of V_{meso}. The process was carried under 40 % RH, which could cause water uptake, leading to rearrangement of the aerogel network, resulting in loss of A_{BET} and changes in the pore size distribution [50]. In the case of γ-rays (*STA_ γ-rays*), the treatment was also unsuccessful since A_{BET} resulted below the expected value for an aerogel, as well as higher D_P and V_{macro} percentage compared to the *STA_Blank* sample. This effect could be the result of a pore collapse, that was also reported in the case of collagen sponges sterilized through γ-rays (from 65 μm to 390 μm) [51].

In the case of the sterilized alginate aerogels (Fig. 3B), $scCO_2$ sterilization under a *static* regime (*ALG_scCO₂St*) caused an important decrease on A_{BET} value as well as an increase in D_P and in the percentage of V_{meso}, However, subjecting the aerogels to a fresh flow of CO_2 (*ALG_scCO₂Dy* and *ALG_scCO₂Co*) allowed to preserve the textural properties of the untreated aerogels with a certain increase in D_P and in the percentage of V_{meso}. The increase in mesopore volume contribution was attributed to CO_2 flow inducing the growth of the mesopore sizes and the micropore coalescence forming new mesopores [27]. The samples treated with EO (*ALG_EO*) exhibited a significative decrease in A_{BET} and D_P compared to *ALG_Blank*, but still within accepted ranges for biopolymeric aerogels. The samples treated with γ-rays exhibited low values of A_{BET}, an acceptable D_P alongside an important increase on the V_{meso} percentage, which is a result of the collapse of the smaller pores as was also observed with starch samples subjected to the same

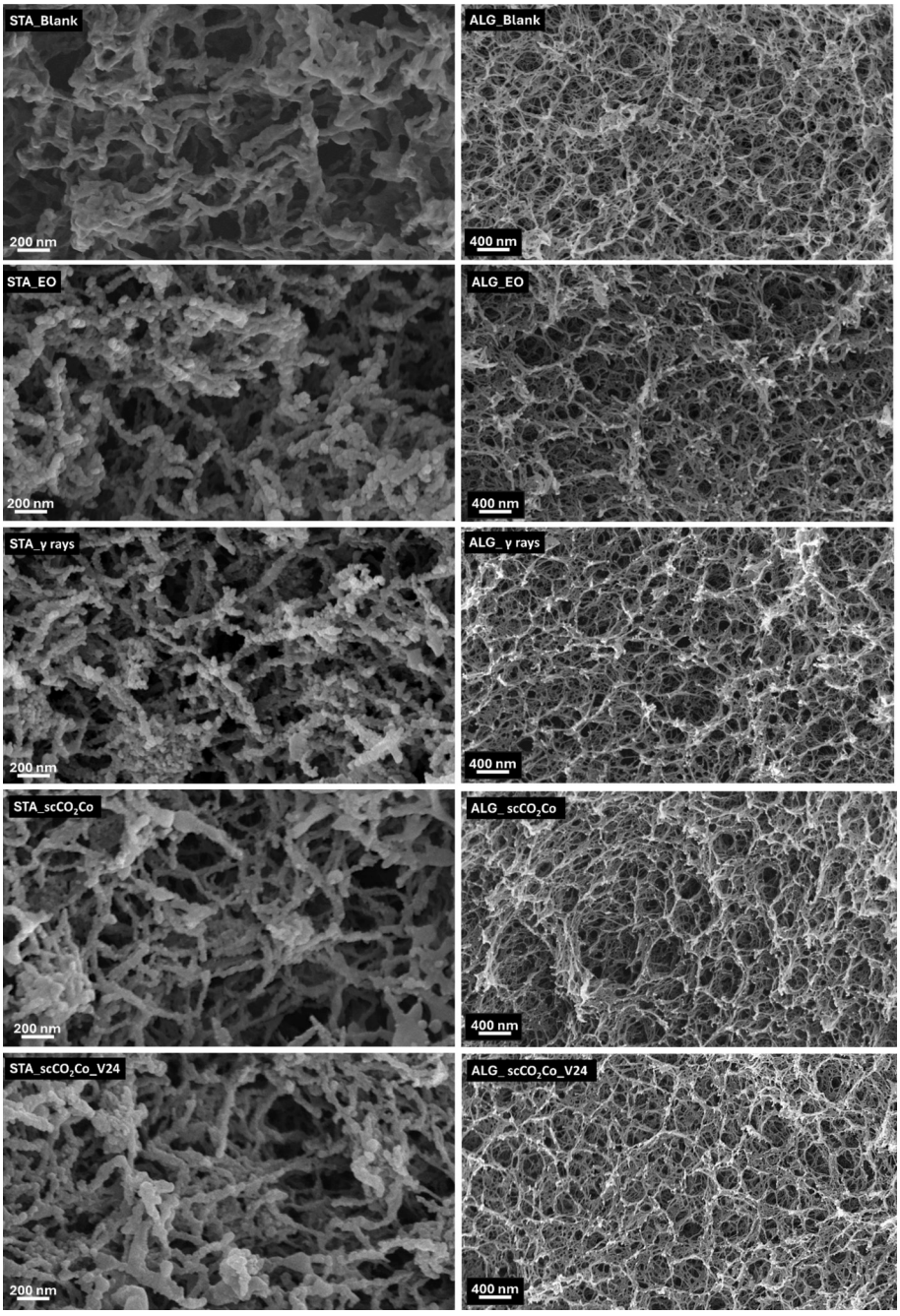

Fig. 4. SEM images of blank and sterilized starch (left column) and alginate (right) aerogels.

sterilization technique.

The SEM images of blank starch and alginate aerogels (*STA_Blank* and *ALG_Blank*) (Fig. 4) exhibited the typical structure of polysaccharide aerogels: a fibrous, open, and highly porous network. The predominance of macropores over mesopores is evident, in agreement with the N_2 adsorption-desorption analysis. However, SEM is not a reliable technique for pore size estimation due to frequent irregular cuts during sample sectioning and the presence of angled surfaces, which compromise measurement accuracy [52]. The fibers in *STA_Blank* aerogels were closely connected to others. Aerogels sterilized by $scCO_2$ with the

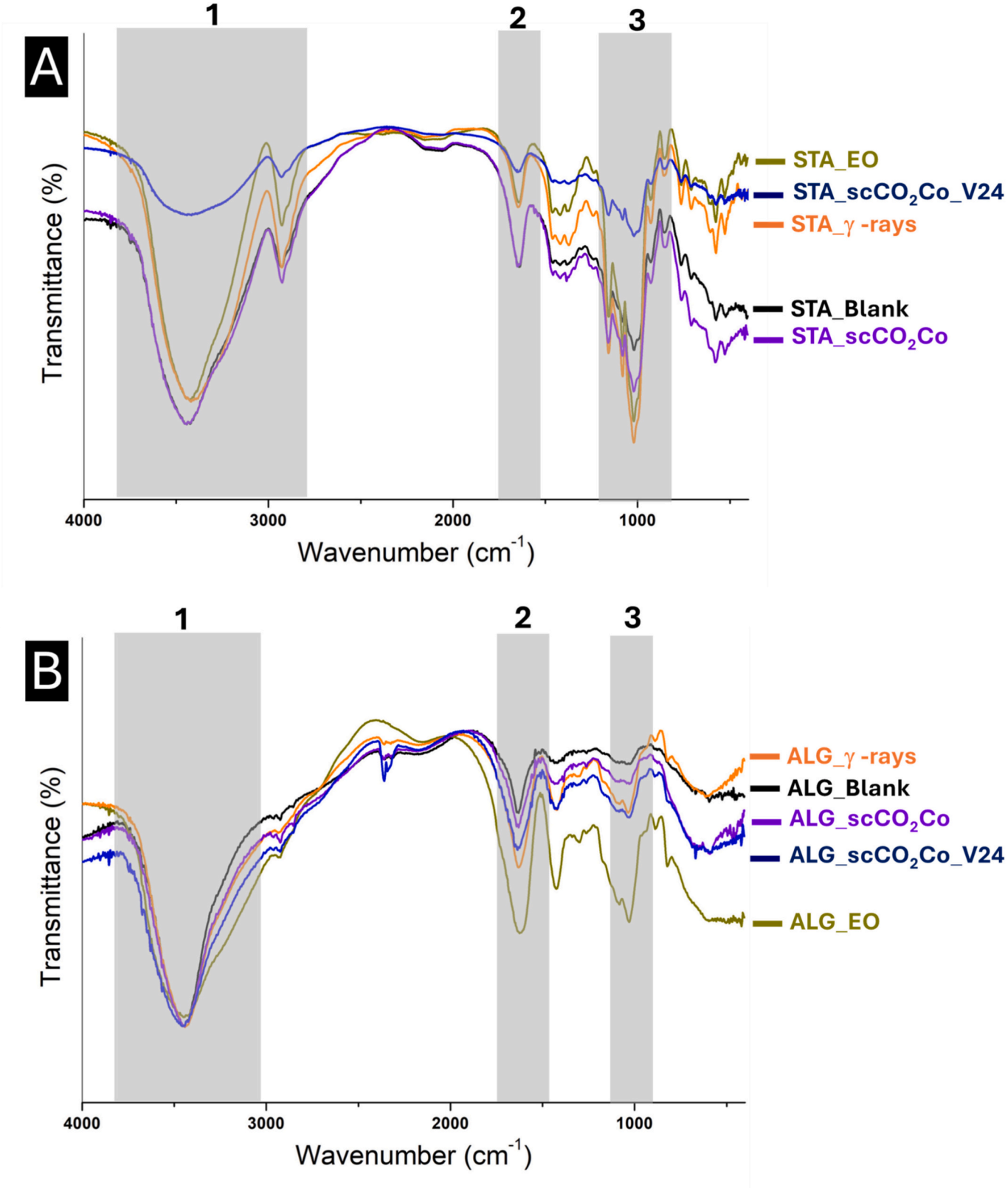

Fig. 5. FTIR spectra of (A) starch and (B) alginate aerogels before and after being treated with the different sterilization procedures.

combined regime (*STA_scCO$_2$Co* and *ALG_scCO$_2$Co*) exhibited a structure similar to the blank samples, as expected from the N_2 adsorption-desorption analysis. In contrast, aerogels sterilized with EO (*STA_EO* and *ALG_EO*) had a porous network with broken fibers, being the fiber damage more evident in the alginate aerogel. This effect of EO sterilization is consistent with the increase in V_{macro} observed in Fig. 3 and was also reported for other fibrous structures such as in medical devices [15,33,38,53]. Agglomerated fibers were also observed in aerogels treated with γ-rays (*STA_γ-rays* and *ALG_γ-rays*), being this effect again more pronounced in the case of alginate fibers, which could form new mesopores with small diameters. This phenomenon has likewise been reported for facemasks sterilized by γ-rays [33]. Overall, these results suggest that the commonly used sterilization techniques in the medical field (EO and γ-rays) are not suitable for alginate or starch aerogels, as they compromise the structural integrity of the material. In contrast, scCO$_2$ sterilization procedures, especially those treatments using a fresh CO$_2$ flow, were more favorable. Particularly, the *combined* regime was the most effective method in preserving the morphological properties of both polysaccharide aerogels (*STA_scCO$_2$Co* and *ALG_scCO$_2$Co*).

3.3. Chemical characterization of aerogels

3.3.1. Fourier-Transform Infrared spectroscopy characterization

FTIR spectra of sterilized and untreated starch and alginate aerogel samples (Fig. 5) show no significant differences between the sterilization treatments. In the case of starch aerogel samples (Fig. 5A), the region A1 had a broad O—H stretching band at 3200–3400 cm^{-1}, attributed to hydrogen-bonded hydroxyl groups, along with C—H stretching peaks near 2920–2940 cm^{-1}, characteristic of the glucose rings [46,54]. The C—O bending associated with the OH group shows a band at 1595–1625 cm^{-1} (region A2). The region A3 displayed strong C–O–C (glycosidic link) absorption bands between 1000 and 1150 cm^{-1}, mainly centered at 1020–1080 cm^{-1}, together with C—O stretching peaks in the 930–1155 cm^{-1} range, associated with the C-O-C pyranose ring and glycosidic bonds [54]. In the case of alginate aerogel samples (Fig. 5B), no significant differences were observed in the characteristic bands of alginate (O—H stretching at 3200–3400 cm^{-1} in region B1, asymmetric COO$^-$ stretching at 1595–1625 cm^{-1} in region B2, and C—O stretching/glycosidic vibrations at 1020–1100 cm^{-1} in region B3) [27,55].

3.3.2. Nuclear Magnetic Resonance (NMR) spectroscopy characterization

Quantitative proton nuclear magnetic resonance spectroscopy (^{1}H qNMR) spectroscopy was applied to elucidate the chemical structure of starch and alginate aerogels and evaluate the effect of each processing step, from the raw material to the sterilization of the final aerogels. ^{1}H qNMR is a non-destructive and non-invasive analytical technique with high sensitivity and specificity for the quantification of excipients in pharmaceutical products [30,56]. The approach does not require complex sample manipulation or chemical modifications and represents a robust and reliable alternative to traditional analytical techniques.

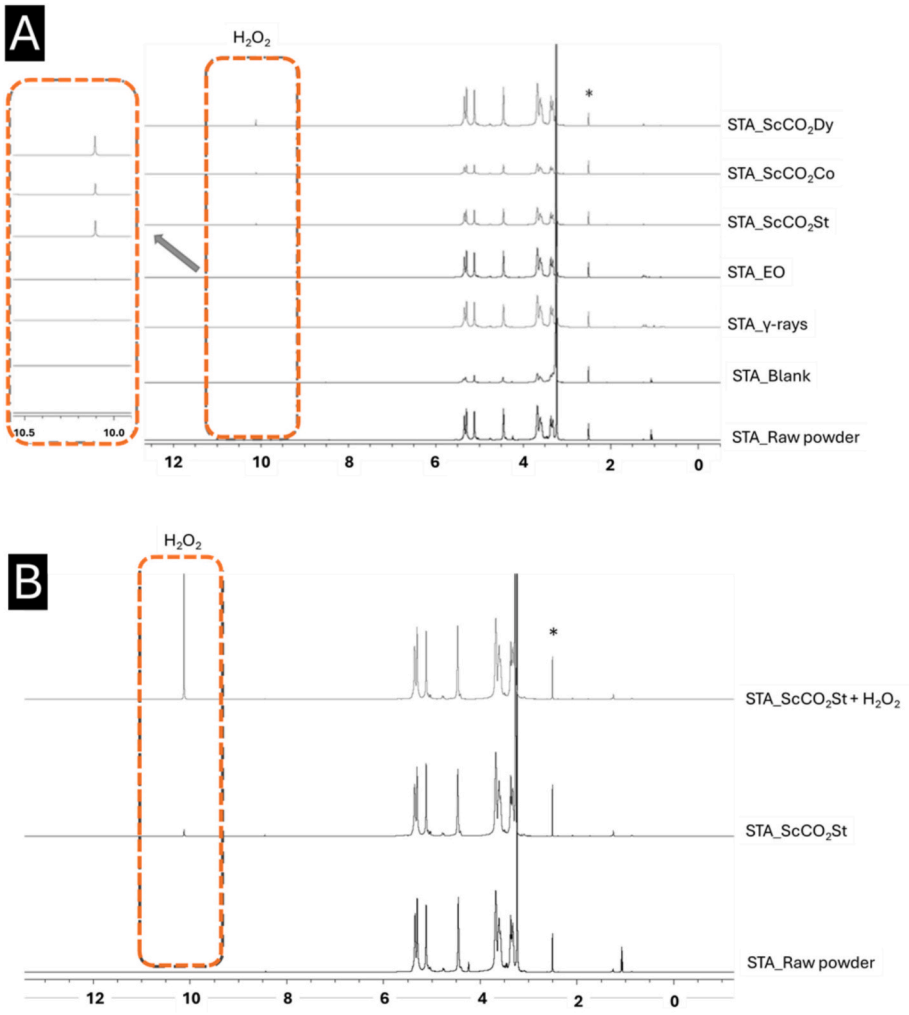

Fig. 6. ^{1}H qNMR @ 600 MHz, 320 K of (A) starch samples for comparison between sterilization procedures. (B) Starch samples compared for the elucidation of H_2O_2 signal after addition of 0.1 μL H_2O_2. Enlarged region referred to a vertical expansion of H_2O_2 resonance. Signal marked with the asterisk is DMSO.

The ^{1}H qNMR spectra for starch samples (Fig. 6A) evidenced the typical resonances of native maize starch dissolved in d-DMSO, a polymer made of amylose and amylopectin with the 2–6 protons identified in the 3.21–3.89 ppm region [57,58]. The signals of anomeric α-(1,4) protons were assigned to the region of 5.0–5.2 ppm, while the α-(1,6) protons associated with the branched structure of amylopectin, were assigned to 4.7–4.8 ppm signals. Since no discernible differences were revealed in the characteristic range of starch, both manufacturing and the sterilization processes seem not to induce any chemical alterations in the polymeric structure of starch. However, the samples subjected to $scCO_2$ sterilization procedures exhibited a new extremely sharp signal at 10.1 ppm that was associated with the sterilization additive, i.e. H_2O_2 [59,60]. To confirm this hypothesis, 0.1 μL of the sterilization additive (H_2O_2 35 % w/w), was added in a NMR tube containing a dissolved sterilized starch aerogel (*STA_scCO₂St*). This resulted in a marked increase in the signal intensity at 10.1 ppm in the proton spectrum (Fig. 6B), thereby supporting the initial assumption.

A ^{1}H-qNMR protocol was used for H_2O_2 quantification in the $scCO_2$ sterilized aerogels. This analytical approach was previously used to measure H_2O_2 concentrations from 10^{-3} to 10 M in cosmetic and cleaning products, such as hair sprays, nail treatments, H_2O_2 solutions for disinfection and chemical reagents and polymers commonly used as pharmaceutical excipients [59,61,62]. The internal standard validation evidences a strong agreement in both the accuracy of the adopted methodology and the consistency of data obtained with both internal and external standards (Table S1). The results of the H_2O_2 quantification in the $scCO_2$ sterilized aerogels are presented in Table 2. According with ^{1}H qNMR spectra, when starch aerogels were treated under optimal conditions (*STA_scCO₂Co*), the sterilized starch sample retained 183 ppm of H_2O_2 equivalent to roughly 13.8 % of the H_2O_2 added for achieving sterility levels.

To validate the ^{1}H qNMR method, H_2O_2 quantification was also performed using an internal standard solution on randomly selected samples. The validation results for the external and internal standards are reported in Table S2, revealing strong agreement and thus confirming the accuracy and reliability of the employed analytical methodology.

The ^{1}H qNMR was also applied to alginate samples (Fig. 7). ^{1}H qNMR was recorded in DMSO instead of D_2O for a precise quantification of H_2O_2, considering the abovementioned results for starch samples. Although water is a better solvent for alginate, H_2O_2 molecules would fast decompose in aqueous media, resulting in a broad and poorly defined signal unsuitable for quatification. Some changes were appreciated between the raw powder and the aerogel samples, but these changes could be attributed to the hard solubility of the samples in DMSO. Moreover, EO and γ-rays sterilization induced polymer chain scission with new signals in the 4–6 ppm range [63]. Similarly to starch samples, the ^{1}H qNMR spectrum of the $scCO_2$ sterilized sample displayed a sharp signal at 10.1 ppm and assigned to H_2O_2. As observed for starch aerogels, *ALG_scCO₂Co* sample treated under optimal $scCO_2$ sterilization conditions, showed remnants of the H_2O_2 added for sterilization (9.0 %) within the polymeric matrix (Table 2).

Table 2
Residual H_2O_2 contents on sterile starch and alginate aerogels through $scCO_2$ technology before and after aeration treatments. Conditions in bold text correspond to the selected optimized conditions.

Sample	External standard [H_2O_2] ppm*
STA_scCO₂Co	183
STA_scCO₂Co_V2	509
STA_scCO₂Co_V24	**132**
STA_scCO₂Co_2.5bar	178
STA_scCO₂Co_50bar	238
ALG_scCO₂Co	121
ALG_scCO₂Co_V2	148
ALG_scCO₂Co_V24	**74**
ALG_scCO₂Co_2.5bar	148
ALG_scCO₂Co_50bar	61

* Calculated with respect to the solubilized amount of aerogel in 0.75 mL of d-DMSO, using an external H_2O_2 standard solution ([H_2O_2] = 6.13 mM).

3.3.3. Amylose-to-amylopectin ratio determination of starch aerogels

The amylose-to-amylopectin ratio for the aerogel samples (Table 3) showed that sterilization treatments increased this ratio to different degrees. The branched structure of amylopectin is significantly more sensitive to breaking than the linear structure of amylose [64]. As a result, the amylose-to-amylopectin ratio increased due to amylopectin content decreases. This change was more noticeable in the samples treated with $scCO_2$, regardless of the exposure regime. Although this effect was firstly attributed to the oxidative nature of H_2O_2, the samples treated only in the presence of water (*STA_scCO₂Co_1+1.5_0*) also showed changes in the amylose-to-amylopectin ratio. Nevertheless, this aerogel sample exhibited an intermediate value with a non-significant difference compared to aerogels processed under other supercritical conditions or even under γ-rays. This suggests that under a $scCO_2$ and water mixture environment structural rearrangements could be induced, and that such effects are further enhanced in the presence of H_2O_2. In agreement with literature, $scCO_2$ has been reported as a plasticizer, increasing the mobility of starch chains within the amorphous regions [65] thereby allowing water diffusion and promoting partial disruption of crystalline domains, leading to a more disordered starch structure [66].

3.3.4. Gel permeation chromatography of sterilized samples

The GPC molecular weight distributions are shown in Fig. SI.1 while the analysis of the relevant peaks of starch and alginate samples are presented in Table 4 and Table 5 respectively.

The results obtained after the analysis of *STA_Blank* aerogel presented one macromolecular population (Fig. SI.1A) and indicate a homogeneous polymer with a high degree of polymerization (Table 4). The fact that the values for Mn and Mw are close to each other suggests a narrow molecular weight distribution. This could mean that the weight proportion of the small amylose molecules is similar to that of the large amylopectin molecules. This finding is consistent with the measured amylose-to-amylopectin ratio determination (Table 3) of 44.4 %. The starch aerogels sterilized by the $scCO_2$ treatment under the *combined* regime (*STA_scCO₂Co*) appear to selectively degrade short branches or fragments of amylopectin, while preserving long linear chains (amylose), since there was a single macromolecular population with higher values of Mn, Mw and amylose-to-amylopectin weight ratio. In contrast, the samples subjected to EO and γ-rays (*STA_EO* and *STA_γ-rays*) exhibited bimodal molecular weight distributions suggesting the presence of two main macromolecular populations. The results reflected increased heterogeneity and a reduced degree of polymerization, evidencing partial degradation via chain scission. Based on the amylose-to-amylopectin ratio results, this suggests that amylopectin was more strongly affected, as its branched α-(1 → 6)-linkages are more susceptible to break under oxidative or radiolytic conditions [64].

The chromatograms of alginate samples (Fig. SI.1B) revealed two macromolecular populations in all alginate samples, corresponding to high- (peak 1) and low-molecular weight (peak 2) fractions. The raw alginate powder (*ALG_Raw Powder*) exhibited the highest molecular weights and broad Đ, typical of untreated polysaccharides. The fabrication of the unsterilized aerogel induced a partial degradation of the polymer since *ALG_Blank* sample showed a noticeable decrease in molecular weight and Đ.

For Peak 1, a clear decrease in both the Mn and Mw molecular weights was observed after the aerogel fabrication and sterilization compared with the raw powder. All the samples treated with $scCO_2$ (*static*, *dynamic*, and *combined* regimes) showed a less severe depolymerization effect. Specially, the combined regime with additive,

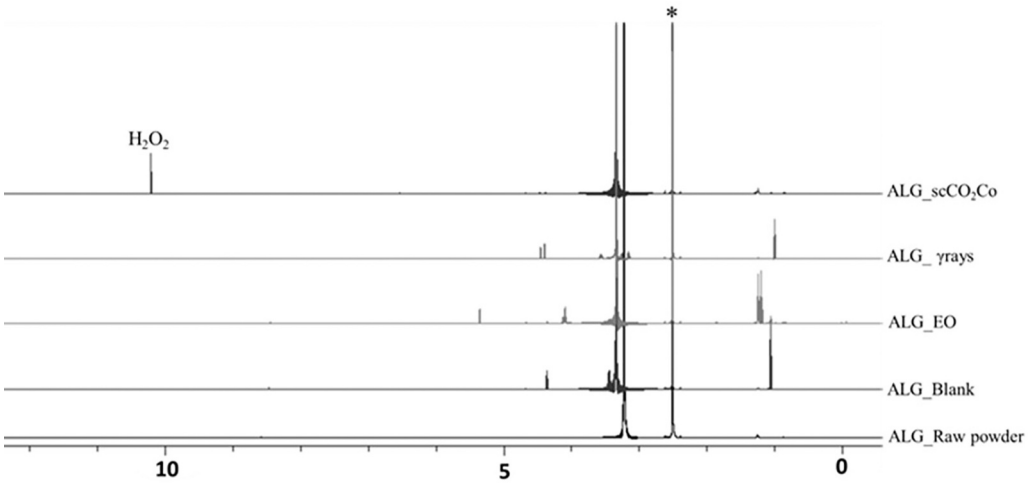

Fig. 7. ^{1}H qNMR @ 600 MHz, 320 K of alginate samples for comparison between sterilization procedures. Signal marked with the asterisk is DMSO.

Table 3
Amylose-to-amylopectin ratio results of the starch samples before and after the different fabrication and sterilization treatments. Equal letters denoted statistically homogeneous groups.

Sample	Ratio amylose-to-amylopectin (%)
STA_Raw powder	46.3 ± 0.9[a]
STA_Blank	44.4 ± 2.5[a]
STA_EO	48.0 ± 3.3[a]
STA_γrays	50.4 ± 1.6[a,b]
STA_scCO$_2$St	65.3 ± 5.0[c]
STA_scCO$_2$Dy	63.6 ± 5.6[c]
STA_scCO$_2$Co	66.1 ± 1.9[c]
STA_scCO$_2$Co_1+1.5_0	60.9 ± 5.9[b,c]

Table 4
Gel permeation chromatography (GPC) results of blank (*STA_Blank*) and sterilized starch aerogel samples. Number-average molecular weight (Mn), weight-average molecular weight (Mw), dispersity (Đ), and degree of polymerization are reported for each aerogel sample.

Sample	*Mn* (kDa)	*Mw* (kDa)	Đ	DP
STA_Blank	224.31	351.80	1.57	1383.4
STA_EO	149.83	473.13	3.16	924.1
STA_γ rays	155.70	398.95	2.56	960.2
STA_scCO$_2$Co	266.12	376.28	1.41	1641.3
STA_scCO2Co_V24	249.20	370.70	1.49	1537.0

ALG_scCO$_2$Co, which showed intermediate values suggesting a balance between sterilization efficiency and polymer integrity, similarly as was demonstrated in the textural analysis. The most pronounced degradation occurred in the samples sterilized with EO and γ rays (*ALG_EO* and *ALG_γ rays*) with a decrease of 81 % and 98 %, respectively, and a marked reduction in the degree of DP, consistent with the oxidative behavior of EO and the radical-induced breakage of glycosidic bonds after γ-rays treatment [67]. This degradation effect was also observed in raw alginates after being irradiated under different doses of γ-rays [68]. The raw alginate subjected to 60 kGy exhibited an important reduction (*ca.* 84.6 %) on Mw.

For Peak 2, corresponding to the lower-molecular-weight fraction, all samples exhibited narrower dispersity values (Đ ≈ 1.0–1.3). The aerogels treated with scCO$_2$ technology maintained similar values to the untreated counterparts while the decrease in Mn and Mw was again more pronounced for EO and γ-ray treatments.

In both peaks could be observed that the sample treated in the absence of H_2O_2 (*ALG_scCO$_2$Co_1+1.5_0*) had values closer to *ALG_Blank*, in except of DP value, which could be related to changes on the structural water of the polysaccharide. Overall, although all sterilization methods reduced the alginate molecular weight, oxidant-assisted scCO$_2$ treatments provided the best balance between sterilization efficiency and preservation of polymer integrity, yielding aerogels with intermediate molecular weights and homogeneous molecular distributions.

Table 5
Gel permeation chromatography (GPC) results of alginate raw powder (*ALG_Raw Powder*), blank aerogel (*ALG_Blank*), and sterilized aerogel samples. Number-average molecular weight (Mn), weight-average molecular weight (Mw), dispersity (Đ), and degree of polymerization (DP) are reported for each sample and for the two macromolecular population observed (peak 1 and 2).

Sample	*Mn* (kDa)	*Mw* (kDa)	Đ	DP
Peak 1				
ALG_Raw Powder	396.81	2400.63	6.050	12,003
ALG_Blank	212.41	1121.05	5.278	5605
ALG_EO	73.17	156.97	2.145	785
ALG_γ rays	82.77	186.22	2.250	931
ALG_scCO$_2$St	71.79	136.64	1.903	683
ALG_scCO$_2$Dy	67.71	138.52	2.046	693
ALG_scCO$_2$Co	79.64	218.78	2.747	1094
ALG_scCO2Co_1+1.5_0	146.78	834.29	5.684	4171
Peak 2				
ALG_Raw Powder	9.19	10.85	1.180	54
ALG_Blank	7.64	8.74	1.144	44
ALG_EO	4.66	5.90	1.266	29
ALG_γ rays	4.59	4.96	1.082	25
ALG_scCO$_2$St	4.67	4.76	1.018	24
ALG_scCO$_2$Dy	4.44	4.87	1.096	24
ALG_scCO$_2$Co	3.90	4.32	1.108	22
ALG_scCO2Co_1+1.5_0	5.37	5.86	1.091	29

3.4. Aeration effect and in vitro cell test of sterilized polysaccharide aerogels

The aerogel samples obtained under the optimal operational sterilization conditions (*STA_scCO$_2$Co* and *ALG_scCO$_2$Co*) were tested in terms of biocompatibility with NIH-3T3 cell line (Fig. 8). This cell line is widely accepted for cytotoxicity testing because it mimics connective-tissue responses and minimizes false negatives [69]. On both materials, there was no cytotoxic effect detected for the *Blank* samples, although the mandatory sterility condition for using these materials as

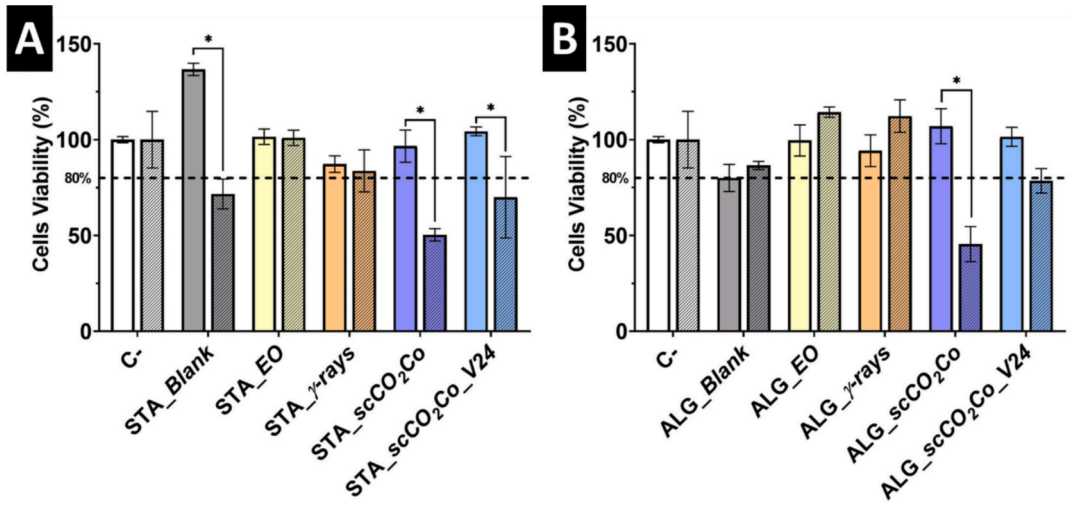

Fig. 8. Cell viability studies of (A) starch and (B) alginate aerogels. Light color corresponds to the results after 24 h of exposure of the cells to the samples, and dark color corresponds to the results after 48 h of exposure. Asterisk (*) denotes statistically significant difference between 24 h and 48 h results.

biomedical devices was not accomplished. The aerogels treated under the supercritical sterilization method were sterile at SAL-6 levels but cytotoxic after 48 h of contact with the cells. This cytotoxicity was related to the presence of H_2O_2 in the samples (cf. Section 2.3). In contrast, the sterility with EO and γ rays did not compromise the biocompatibility of both polysaccharide aerogels as long as the aeration and the dose were controlled in normalized procedures to avoid toxic residues. An analog aeration procedure was then adapted for the supercritical sterilization treatment to pursue the biocompatibility of the sterilized material.

The H_2O_2 quantification was performed on *STA_scCO$_2$Co* and *ALG_scCO$_2$Co* before and after being subjected to different aeration treatments (Table 2). For starch aerogels, it was observed that the sample with less concentration of H_2O_2 was the one subjected to 24 h of vacuum (*STA_scCO2Co_V24*) with a value of 132 ppm of H_2O_2. Similarly, for alginate sterilized samples, the lowest H_2O_2 content was observed when the aerogels were subjected under vacuum for 24 h (*ALG_scCO2Co_V24*) or exposed to 50 bar of CO_2 (*ALG_scCO2Co_50bar*). Shorter vacuums times (*STA_scCO2Co_V2* and *ALG_scCO2Co_V2*) or atmospheres at lower CO_2 pressures (*STA_scCO2Co_2.5bar* and *ALG_scCO2Co_2.5bar*) had a negligible effect on H_2O_2 content reduction in the aerogel backbone. Since for both polysaccharides the lowest amount of H_2O_2 was obtained after exposing the samples of 24 h of vacuum, *STA_scCO$_2$Co_V24* and *ALG_scCO$_2$Co_V24* aerogels were selected as the optimal aeration conditions for obtaining sterile aerogels.

To verify that the vacuum treatment did not alter the functionality of the sterilized aerogel (*STA_scCO$_2$Co* and *ALG_scCO$_2$Co*), the samples subjected to 24 h of vacuum (*STA_scCO$_2$Co_V24* and *ALG_scCO$_2$Co_V24*) were characterized by SEM and FTIR (Figs. 3 and 4). These analyses revealed no significant textural or chemical differences compared with the non-aerated sterilized counterparts (*STA_scCO$_2$Co* and *ALG_scCO$_2$Co*). As a preliminary and conservative toxicological screening, the Margin of Safety (MoS) was estimated following ISO 10993-17 using the equation MoS = TI / Exposure, with a conservative Tolerable Intake (TI) of 0.4 mg/(kg·day) derived from repeated-dose NOAEL data (~40 mg/(kg·day) in rats) and standard uncertainty factors applied (×100) [70]. Exposure was calculated under a worst-case scenario, assuming a 70 kg patient and complete release of the total H_2O_2 content quantified by ^{1}H NMR from 1 g of aerogel within 24 h. Under these conditions, the *STA_scCO$_2$Co_V24* and *ALG_scCO$_2$Co_V24* samples exhibited MoS values of 2.83 and 5.00, respectively, exceeding the ISO 10993-17 acceptance criterion (MoS > 1) and supporting the toxicological acceptability of the materials within the scope of this study. Finally, the cell viability test confirmed the additional advantage of these aerogel samples in maintaining biocompatibility even after 48 h of contact with cells.

4. Conclusions

The effectiveness of $scCO_2$ technology in the sterilization of polysaccharide aerogels in comparison to conventional EO and gamma radiation treatments was herein demonstrated. Sterilization protocols were developed in which exposure time and additive concentration were identified as the critical variables for reaching SAL-6 sterility. The optimal conditions were set at 2.5 h of treatment and an additive concentration of 1330 ppm of H_2O_2. Regarding the textural and chemical properties of the sterilized aerogels, $scCO_2$ exposure regime had a clear effect on the porous structure of the aerogels, with supercritical sterilization under a combined $scCO_2$ regime (i.e. 1 h of *static* regime followed by 1.5 h of *dynamic* regime) allowing a balance between the effectiveness of the process and the preservation of the original properties of the material. In contrast, conventional EO and gamma methods significantly altered the structure of the aerogels. ^{1}H qNMR results showed that an aeration through a vacuum treatment of 24 h after supercritical sterilization reduced the amount of H_2O_2 by *ca.* 30 and 40 % in starch and alginate aerogels, respectively. This post-sterilization vacuum treatment was a key step to ensure the cellular compatibility of aerogels intended for regenerative medicine purposes. The supercritical methodology herein proposed can be extended to other materials and purposes and can open the possibility of the safe reuse and recycling of nanostructured materials, from polysaccharides to other complex materials through their microbial inactivation.

CRediT authorship contribution statement

María Carracedo-Pérez: Writing – review & editing, Writing – original draft, Methodology, Investigation. **Antonella Caterina Boccia:** Writing – review & editing, Writing – original draft, Methodology, Investigation. **Inés Ardao:** Writing – review & editing, Methodology, Investigation. **Cláudia P. Passos:** Writing – review & editing, Methodology. **Víctor Santos-Rosales:** Methodology, Investigation. **Beatriz Santos:** Methodology, Investigation. **Fabio Bernardo:** Methodology. **María Blanco-Vales:** Writing – review & editing, Methodology. **Beatriz Magariños:** Writing – review & editing, Writing – original draft, Supervision, Methodology, Investigation, Funding acquisition, Conceptualization. **Carlos A. García-González:** Writing – review & editing, Writing – original draft, Supervision, Methodology, Investigation, Funding acquisition, Conceptualization.

Declaration of competing interest

All authors disclose no actual or potential conflict of interest related with any financial and personal relationships with other people or organizations that could inappropriately influence, or be perceived to influence, this work.

Acknowledgements

This work was funded by MICIU/AEI/10.13039/501100011033 [grants PID2023-151340OB-I00 and PDC2022-133526-I00], Xunta de Galicia [ED431C2022/2023], GAIN [Vinnovate call, AEROCARE, IN848G 2024/01], ERDF/EU and European Union NextGeneration EU/PRTR. Work carried out in the framework of the ECO-AERoGELS COST Innovators' Grant (ref. IG18125) and funded by the European Commission. Authors are grateful for technical support to: Alberto Giacometti Schieroni for Light Scattering on starch samples. The financial support from PT national funds (FCT/MCTES) of LAQV-REQUIMTE/University of Aveiro (UID/50006 -Laboratório Associado para a Química Verde - Tecnologias e Processos Limpos) research unit is acknowledged. FCT is also thanked for Individual Call to Scientific Employment Stimulus contract CPP (CEECIND/01873/2017; DOI: 10.54499/CEECIND/00813/2017/CP1459/ CT0053).

Appendix A. Supplementary data

Supplementary data to this article can be found online at https://doi.org/10.1016/j.bioadv.2025.214698.

Data availability

Data will be made available on request.

References

[1] G. Horvat, M. Pantić, Ž. Knez, Z. Novak, A brief evaluation of pore structure determination for bioaerogels, Gels 8 (2022) 438, https://doi.org/10.3390/gels8070438.
[2] H. Fan, B. Xue, J. Lu, T. Sun, Q. Zhao, Y. Liu, M. Niu, S. Yu, Y. Yang, L. Zhang, Recent advances of bioaerogels in medicine: preparation, property and application, Int. J. Biol. Macromol. 291 (2025) 139144, https://doi.org/10.1016/j.ijbiomac.2024.139144.
[3] I. Lázár, L. Čelko, M. Menelaou, Aerogel-based materials in bone and cartilage tissue engineering—A review with future implications, Gels 9 (2023) 746, https://doi.org/10.3390/gels9090746.
[4] A. Iglesias-Mejuto, B. Magariños, T. Ferreira-Gonçalves, R. Starbird-Pérez, C. Álvarez-Lorenzo, C.P. Reis, I. Ardao, C.A. García-González, Vancomycin-loaded methylcellulose aerogel scaffolds for advanced bone tissue engineering, Carbohydr. Polym. 324 (2024) 121536, https://doi.org/10.1016/j.carbpol.2023.121536.
[5] T. Duong, M. Vivero-Lopez, I. Ardao, C. Alvarez-Lorenzo, A. Forgács, J. Kalmár, C. A. García-González, Alginate aerogels by spray gelation for enhanced pulmonary delivery and solubilization of beclomethasone dipropionate, Chem. Eng. J. 485 (2024) 149849, https://doi.org/10.1016/j.cej.2024.149849.
[6] H.M. Alkhalidi, A.A. Alahmadi, W.Y. Rizg, E.B. Yahya, A.K. H.P.S., R.Y. Mushtaq, M.Y. Badr, A.Y. Safhi, K.M. Hosny, Revolutionizing cancer treatment: biopolymer-based aerogels as smart platforms for targeted drug delivery, Macromol. Rapid Commun. 45 (2024) 2300687, https://doi.org/10.1002/marc.202300687.
[7] N. Guo, Y. Xia, W. Zeng, J. Chen, Q. Wu, Y. Shi, G. Li, Z. Huang, G. Wang, Y. Liu, Alginate-based aerogels as wound dressings for efficient bacterial capture and enhanced antibacterial photodynamic therapy, Drug Deliv. 29 (2022) 1086–1099, https://doi.org/10.1080/10717544.2022.2058650.
[8] J. Schmier, C. Hulme-Lowe, S. Semenova, J. Klenk, P. Deleo, R. Sedlak, P. Carlson, Estimated hospital costs associated with preventable Health care-associated infections if Health care antiseptic products were unavailable, Clin. Outcomes Res. 197 (2016), https://doi.org/10.2147/CEOR.S102505.
[9] A. Agarwal, A. Kelkar, A.G. Agarwal, D. Jayaswal, C. Schultz, A. Jayaswal, V. K. Goel, A.K. Agarwal, S. Gidvani, Implant retention or removal for management of surgical site infection after spinal surgery, Glob. Spine J. 10 (2020) 640–646, https://doi.org/10.1177/2192568219869330.
[10] T. Sandle, Regulatory requirements and good manufacturing practices (GMP), in: Sterility, Sterilisation and Sterility Assurance for Pharmaceuticals, Elsevier, 2025, pp. 55–74 (ISBN 978-0-443-36436-5.).
[11] M. Carracedo-Pérez, B. Magariños, C.A. García-González, Strategies for the sterilization of polymeric biomaterials, in: Polymeric Materials for Biomedical Implants, Elsevier, 2024, pp. 547–583 (ISBN 978-0-323-99690-7.).
[12] W.J. Rogers, Chapter 2: steam and dry heat sterilization of biomaterials and medical devices, in: Sterilisation of Biomaterials and Medical Devices, Elsevier, 2012, pp. 20–55 (ISBN 978-1-84569-932-1.).
[13] W.J. Rogers, Chapter 7: Sterilisation techniques for polymers, in: Sterilisation of Biomaterials and Medical Devices, Elsevier, 2012, pp. 151–211 (ISBN 978-1-84569-932-1.).
[14] ISO 17665-1:2006 Sterilization of Health Care Products-Moist Heat-Part 1: Requirements for the Development, Validation and Routine Control of a Sterilization Process for Medical Devices, 2006.
[15] A. Pereira, G. Nakka, S. Gupta, Beyond ethylene oxide (EtO): a comprehensive review of sustainable sterilization technologies for medical devices, Biomed. Ther. Lett. 12 (2025) 1161, https://doi.org/10.62110/sciencein.btl.2025.v12.1161.
[16] C. Kirman, A. Li, P. Sheehan, J. Bus, R. Lewis, S. Hays, Ethylene oxide review: Characterization of total exposure via endogenous and exogenous pathways and their implications to risk assessment and risk management, J. Toxicol. Environ. Health Part B 24 (2021) 1–29, https://doi.org/10.1080/10937404.2020.1852988.
[17] J. Whitworth, Ethylene oxide and Salmonella feature in major FSA incidents, Food Safety News, 2022. Available at: https://www.foodsafetynews.com/2022/09/ethylene-oxide-and-salmonella-feature-in-major-fsa-incidents/ (Accessed on 28 Nov 2023).
[18] M. Tohfafarosh, D. Baykal, J.W. Kiel, K. Mansmann, S.M. Kurtz, Effects of gamma and E-beam sterilization on the chemical, mechanical and tribological properties of a novel hydrogel, J. Mech. Behav. Biomed. Mater. 53 (2016) 250–256, https://doi.org/10.1016/j.jmbbm.2015.08.024.
[19] C.R. Harrell, V. Djonov, C. Fellabaum, V. Volarevic, Risks of using sterilization by gamma radiation: the other side of the coin, Int. J. Med. Sci. 15 (2018) 274–279, https://doi.org/10.7150/ijms.22644.
[20] National Academies of Sciences, E, Studies, D. on E. and L, Board, N. and R.S.; Technologies, C. on R.S.A. and A, Radioactive sources and alternative technologies in sterilization, in: Radioactive Sources: Applications and Alternative Technologies, National Academies Press (US), 2021.
[21] C. Health, D. and R., FDA Innovation Challenge 1: Identify New Sterilization Methods and Technologies, Available at:, U.S. Food and Drug Administration, 2019 (Accessed on 02 May 2025), https://www.fda.gov/medical-devices/general-hospital-devices-and-supplies/fda-innovation-challenge-1-identify-new-sterilization-methods-and-technologies.
[22] K.L. Delma, N. Penoy, A.K. Sakira, S. Egrek, R. Sacheli, B. Grignard, M.-P. Hayette, T. Issa Somé, B. Evrard, R. Semdé, et al., Use of supercritical CO_2 for the sterilization of liposomes: study of the influence of sterilization conditions on the chemical and physical stability of phospholipids and liposomes, Eur. J. Pharm. Biopharm. 183 (2023) 112–118, https://doi.org/10.1016/j.ejpb.2023.01.002.
[23] D. Bennet, A.F. Harris, J. Lacombe, C. Brooks, N. Bionda, A.D. Strickland, T. Eisenhut, F. Zenhausern, Evaluation of supercritical CO_2 sterilization efficacy for sanitizing personal protective equipment from the coronavirus SARS-CoV-2, Sci. Total Environ. 780 (2021) 146519, https://doi.org/10.1016/j.scitotenv.2021.146519.
[24] C.S.A. Bento, S. Alarico, N. Empadinhas, H.C. de Sousa, M.E.M. Braga, Sequential $scCO_2$ drying and sterilisation of alginate-gelatine aerogels for biomedical applications, J. Supercrit. Fluids 184 (2022) 105570, https://doi.org/10.1016/j.supflu.2022.105570.
[25] H.K. Ruiz, A. Cabañas, L. Calvo, Sterilisation and virus SARS-CoV-2 inactivation in personal protective equipment with supercritical CO_2, J. Ind. Eng. Chem. (2025), https://doi.org/10.1016/j.jiec.2025.01.041.
[26] V. Santos-Rosales, B. Magariños, R. Starbird, J. Suárez-González, J.B. Fariña, C. Alvarez-Lorenzo, C.A. García-González, Supercritical CO_2 technology for one-pot foaming and sterilization of polymeric scaffolds for bone regeneration, Int. J. Pharm. 605 (2021) 120801, https://doi.org/10.1016/j.ijpharm.2021.120801.
[27] M. Carracedo-Pérez, I. Ardao, C. López-Iglesias, B. Magariños, C.A. García-González, Direct and green production of sterile aerogels using supercritical fluid technology for biomedical applications, J. CO_2 Util. 86 (2024) 102891, https://doi.org/10.1016/j.jcou.2024.102891.
[28] AENOR ISO 11135:2014, Sterilization of Health Care Products-Ethylene Oxide-Part 1:Requirements for the Development, Validation and Routine Control of a Sterilization Process for Medical Devices, 2014.
[29] AENOR ISO 11137-1:2006, Sterilization of Health Care Products-Radiation-Part 1: Requirements for Development, Validation and Routine Control of a Sterilization Process for Medical Devices, 2006.
[30] S.K. Bharti, R. Roy, Quantitative 1H NMR spectroscopy, TrAC Trends Anal. Chem. 35 (2012) 5–26, https://doi.org/10.1016/j.trac.2012.02.007.
[31] A.C. Boccia, G. Scavia, I. Schizzi, L. Conzatti, Biobased cryogels from enzymatically oxidized starch: functionalized materials as carriers of active molecules, Molecules 25 (2020) 2557, https://doi.org/10.3390/molecules25112557.
[32] J. Zhang, S. Burrows, C. Gleason, M.A. Matthews, M.J. Drews, M. LaBerge, Y.H. An, Sterilizing *bacillus Pumilus* spores using supercritical carbon dioxide, J. Microbiol. Methods 66 (2006) 479–485, https://doi.org/10.1016/j.mimet.2006.01.012.
[33] M. Carracedo-Pérez, C. Prieto, M. Blanco-Vales, B. Magariños, C. López-Iglesias, C. A. García-González, Breathing green: sustainable approaches for the reuse of FFP2 facemasks, J. Environ. Chem. Eng. 13 (2025) 118991, https://doi.org/10.1016/j.jece.2025.118991.
[34] V. Warambourg, A. Mouahid, C. Crampon, A. Galinier, M. Claeys-Bruno, E. Badens, Supercritical CO_2 sterilization under low temperature and pressure conditions, J. Supercrit. Fluids 203 (2023) 106084, https://doi.org/10.1016/j.supflu.2023.106084.
[35] C.S.A. Bento, D. Leite Lopes, C. Flora Villarreal, N. Empadinhas, S. Alarico, H.C. de Sousa, M.E.M. Braga, Integrated processes (HPSE+$scCO_2$) to prepare sterilized

alginate-gelatine-based aerogel, Int. J. Pharm. 662 (2024) 124546, https://doi.org/10.1016/j.ijpharm.2024.124546.
[36] F. Zani, C. Veneziani, E. Bazzoni, L. Maggi, G. Caponetti, R. Bettini, Sterilization of corticosteroids for ocular and pulmonary delivery with supercritical carbon dioxide, Int. J. Pharm. 450 (2013) 218–224, https://doi.org/10.1016/j.ijpharm.2013.04.055.
[37] K.L. Delma, N. Penoy, B. Grignard, R. Semdé, B. Evrard, G. Piel, Effects of supercritical carbon dioxide under conditions potentially conducive to sterilization on physicochemical characteristics of a liposome formulation containing apigenin, J. Supercrit. Fluids 179 (2022) 105418, https://doi.org/10.1016/j.supflu.2021.105418.
[38] V. Santos-Rosales, C. López-Iglesias, A. Sampedro-Viana, C. Alvarez-Lorenzo, S. Ghazanfari, B. Magariños, C.A. García-González, Supercritical CO_2 sterilization: an effective treatment to reprocess FFP3 face masks and to reduce waste during COVID-19 pandemic, Sci. Total Environ. 826 (2022) 154089, https://doi.org/10.1016/j.scitotenv.2022.154089.
[39] J.D. Hemmer, M.J. Drews, M. LaBerge, M.A. Matthews, Sterilization of bacterial spores by using supercritical carbon dioxide and hydrogen peroxide, J. Biomed. Mater. Res. B Appl. Biomater. 80B (2007) 511–518, https://doi.org/10.1002/jbm.b.30625.
[40] A. Bernhardt, M. Wehrl, B. Paul, T. Hochmuth, M. Schumacher, K. Schütz, M. Gelinsky, Improved sterilization of sensitive biomaterials with supercritical carbon dioxide at low temperature, PloS One 10 (2015) e0129205, https://doi.org/10.1371/journal.pone.0129205.
[41] C. Blazejewski, F. Wallet, A. Rouzé, R. Le Guern, S. Ponthieux, J. Salleron, S. Nseir, Efficiency of hydrogen peroxide in improving disinfection of ICU rooms, Crit. Care 19 (2015) 30, https://doi.org/10.1186/s13054-015-0752-9.
[42] P.A. Indelicato, 28 - Chemical sterilization techniques for allograft preparation for anterior cruciate ligament reconstruction, in: C.C. Prodromos (Ed.), The Anterior Cruciate Ligament, Second edition, Elsevier, 2018, pp. 117–120.e1. ISBN 978–0–323-38962-4.
[43] F. Bounoure, H. Fiquet, P. Arnaud, Comparison of hydrogen peroxide and peracetic acid as isolator sterilization agents in a hospital pharmacy, Am. J. Health-Syst. Pharm. AJHP Off. J. Am. Soc. Health-Syst. Pharm. 63 (2006) 451–455, https://doi.org/10.2146/ajhp040451.
[44] Hydrogen Peroxide - IDLH | NIOSH | CDC, 2014. Available online: https://www.cdc.gov/niosh/idlh/772841.html (accessed on 9 May 2025).
[45] The Dangers of Hydrogen Peroxide in Sterilization and Bio-Decontamination - GazDetect, 2020. Available online: https://en.gazdetect.com/blog/hydrogen-peroxide-sterilization-biodecontamination-dangers (accessed on 11 May 2025).
[46] V. Santos-Rosales, I. Ardao, C. Alvarez-Lorenzo, N. Ribeiro, A. Oliveira, C. García-González, Sterile and dual-porous aerogels scaffolds obtained through a multistep supercritical CO_2-based approach, Molecules 24 (2019) 871, https://doi.org/10.3390/molecules24050871.
[47] M. Guastaferro, E. Reverchon, L. Baldino, Polysaccharide-based aerogel production for biomedical applications: A comparative review, Materials 14 (2021) 1631, https://doi.org/10.3390/ma14071631.
[48] S. Basak, R.S. Singhal, The potential of supercritical drying as a "green" method for the production of food-grade bioaerogels: a comprehensive critical review, Food Hydrocoll. 141 (2023) 108738, https://doi.org/10.1016/j.foodhyd.2023.108738.
[49] G. Leeke, F. Gaspar, R. Santos, Influence of water on the extraction of essential oils from a model herb using supercritical carbon dioxide, Ind. Eng. Chem. Res. 41 (2002) 2033–2039, https://doi.org/10.1021/ie010845z.
[50] V. Santos-Rosales, G. Alvarez-Rivera, M. Hillgärtner, A. Cifuentes, M. Itskov, C. A. García-González, A. Rege, Stability studies of starch aerogel formulations for biomedical applications, Biomacromolecules 21 (2020) 5336–5344, https://doi.org/10.1021/acs.biomac.0c01414.
[51] N. Karipidou, A.-N. Tzavellas, N. Petrou, C. Katrilaka, K. Theodorou, M. Pitou, E. Tsiridis, T. Choli-Papadopoulou, A. Aggeli, Comparative studies of sterilization processes for sensitive medical nano-devices, Mater. Today Proc. 93 (2023) 1–8, https://doi.org/10.1016/j.matpr.2023.03.260.
[52] S.T. Ho, D.W. Hutmacher, A comparison of micro CT with other techniques used in the characterization of scaffolds, Biomaterials 27 (2006) 1362–1376, https://doi.org/10.1016/j.biomaterials.2005.08.035.
[53] M. Zimniewska, H. Witmanowski, A. Kicinska-Jakubowska, A. Jundzill, E. Kwiatkowska, B. Romanowska, L.B. Malinowski, Assessment of the possibility of surgical masks re-use after a sterilization process in the pandemic condition of COVID-19, Text. Res. J. 92 (2022) 3082–3096, https://doi.org/10.1177/00405175211042889.
[54] G. Lozano-Vazquez, J. Alvarez-Ramirez, C. Lobato-Calleros, E.J. Vernon-Carter, N. Y. Hernández-Marín, Characterization of corn starch-calcium alginate xerogels by microscopy, thermal, XRD, and FTIR analyses, Starch 73 (2021) 2000282, https://doi.org/10.1002/star.202000282.
[55] E. Gómez-Ordóñez, P. Rupérez, FTIR-ATR spectroscopy as a tool for polysaccharide identification in edible brown and red seaweeds, Food Hydrocoll. 25 (2011) 1514–1520, https://doi.org/10.1016/j.foodhyd.2011.02.009.
[56] B.W. Diehl, F. Malz, U. Holzgrabe, Quantitative NMR spectroscopy in the quality evaluation of active pharmaceutical ingredients and excipients, Spectrosc. Eur. 19 (2007) 15–19.
[57] A.C. Boccia, A. Pulvirenti, P. Cerruti, T. Silvetti, M. Brasca, Antimicrobial starch-based cryogels and hydrogels for dual-active food packaging applications, Carbohydr. Polym. 342 (2024) 122340, https://doi.org/10.1016/j.carbpol.2024.122340.
[58] M.J. Tizzotti, M.C. Sweedman, D. Tang, C. Schaefer, R.G. Gilbert, New 1H NMR procedure for the characterization of native and modified food-grade starches, J. Agric. Food Chem. 59 (2011) 6913–6919, https://doi.org/10.1021/jf201209z.
[59] P. Charisiadis, C.G. Tsiafoulis, V. Exarchou, A.G. Tzakos, I.P. Gerothanassis, Rapid and direct low micromolar NMR method for the simultaneous detection of hydrogen peroxide and phenolics in plant extracts, J. Agric. Food Chem. 60 (2012) 4508–4513, https://doi.org/10.1021/jf205003e.
[60] Y.B. Monakhova, B.W.K. Diehl, Rapid ^{1}H NMR determination of hydrogen peroxide in cosmetic products and chemical reagents, Anal. Methods 8 (2016) 4632–4639, https://doi.org/10.1039/c6ay00936k.
[61] I. Saraf, V. Kushwah, B. Werner, K. Zangger, A. Paudel, Quantification of hydrogen peroxide in PVP and PVPVA using 1H qNMR spectroscopy, Polymers 17 (2025) 739, https://doi.org/10.3390/polym17060739.
[62] N.A. Stephenson, A.T. Bell, Quantitative analysis of hydrogen peroxide by ^{1}H NMR spectroscopy, Anal. Bioanal. Chem. 381 (2005) 1289–1293, https://doi.org/10.1007/s00216-005-3086-7.
[63] X. Zhang, J. Chen, X. Shao, H. Li, Y. Jiang, Y. Zhang, D. Yang, Structural and physical properties of alginate pretreated by high-pressure homogenization, Polymers 15 (2023) 3225, https://doi.org/10.3390/polym15153225.
[64] F. Zhu, Starch based aerogels: production, properties and applications, Trends Food Sci. Technol. 89 (2019) 1–10, https://doi.org/10.1016/j.tifs.2019.05.001.
[65] J. Ivanovic, S. Milovanovic, I. Zizovic, Utilization of supercritical CO_2 as a processing aid in setting functionality of starch-based materials: Supercritical CO_2 processing of starch, Starch - Stärke 68 (2016) 821–833, https://doi.org/10.1002/star.201500194.
[66] H. Muljana, F. Picchioni, H.J. Heeres, L.P.B.M. Janssen, Supercritical carbon dioxide ($scCO_2$) induced gelatinization of potato starch, Carbohydr. Polym. 78 (2009) 511–519, https://doi.org/10.1016/j.carbpol.2009.05.005.
[67] M.Z.I. Mollah, M.S. Rahaman, M.R.I. Faruque, M.U. Khandaker, H. Osman, S. Alamri, S. Al-Assaf, Effects of radiation sterilization dose on the molecular weight and gelling properties of commercial alginate samples, Front. Mater. 8 (2021), https://doi.org/10.3389/fmats.2021.761995.
[68] H.L.A. El-Mohdy, Radiation-induced degradation of sodium alginate and its plant growth promotion effect, Arab. J. Chem. 10 (2017) S431–S438, https://doi.org/10.1016/j.arabjc.2012.10.003.
[69] V. Sahinturk, S. Kacar, D. Vejselova, H.M. Kutlu, Acrylamide exerts its cytotoxicity in NIH/3T3 fibroblast cells by apoptosis, Toxicol. Ind. Health 34 (2018) 481–489, https://doi.org/10.1177/0748233718769806.
[70] M.L. Weiner, C. Freeman, H. Trochimowicz, J. de Gerlache, S. Jacobi, G. Malinverno, W. Mayr, J.F. Regnier, 13-week drinking water toxicity study of hydrogen peroxide with 6-week recovery period in catalase-deficient mice, Food Chem. Toxicol. 38 (2000) 607–615, https://doi.org/10.1016/S0278-6915(00)00048-X.